Review

Bioengineered Platforms for Detection Of Group-1 Carcinogenic Metals

Akanksha Singh *

Posted Date: 15 January 2024

doi: 10.20944/preprints202401.1006.v1

Keywords: Cancer; toxicity; carcinogenic metals; sensors; microelectronics; biotechnology

Review

Bioengineered Platforms for Detection of Group-1 Carcinogenic Metals

Akanksha Singh

School of Biochemical Engineering, Indian Institute of Technology (BHU) Varanasi, Varanasi, Uttar Pradesh 221005, India; akankshasingh.rs.bce22@iitbhu.ac.in ; Tel.: +91- 9560511004

Abstract: Studies at the molecular, systemic, and epidemiological levels have shown that chronic metal exposure is linked to significant health consequences, including cancer, affecting hundreds of millions worldwide. Subtle and convoluted mechanisms underline metals' toxicity and carcinogenicity. The use of sensors for carcinogenic metals' trace detection is on the rise due to their selectivity, simplicity, and affordability. Biotechnology and microelectronics in the development of sensors have grown complementarily in recent years. This study offers a comprehensive overview of current research and advancements in developing sensors for detecting carcinogenic metals. Here, we have focussed on the developed biosensor platforms for group 1 carcinogens, i.e., arsenic, nickel, cadmium, chromium, and beryllium, along with their brief roles in human carcinogenesis. This review also looks at the importance of sensing such metal exposure in humans from a larger perspective, hoping to influence future research toward early prevention and treatment of illnesses like cancer.

Keywords: Cancer; toxicity; carcinogenic metals; sensors; microelectronics; biotechnology

Introduction

Concerns about the carcinogenicity and toxicity caused by metals are not new. The prominent carcinogens are arsenic (As), nickel (Ni), cadmium (Cd), chromium (Cr), and beryllium (Be). Since the last decade, there has been a growing amount of curiosity to find out more carcinogenic metals polluting the environment. Some of them are iron (Fe), copper (Cu), lead (Pb), and mercury (Hg), as listed by the International Agency for Research on Cancer (IARC) (Lay and Levina, 2013; Rousseau et al., 2005). High doses of iron and copper are carcinogenic, although they are well-controlled and often cause cancer only in animals or individuals with genetic conditions that impair metabolic regulation (Iqbal et al., 2021; Mandil et al., 2020). The phenomenon of cancer induction by metals and their role in environmental health concerns is still poorly understood, despite the growing number of research. These carcinogenic metals are known to cause alterations in normal cellular activity, which may lead to abnormal cell growth and development (Chen et al., 2019). All carcinogenic metals induce cancer via a variety of shared processes that include bio-methylation and the active role of redox-reactive species. Similarly, numerous carcinogenic metals may affect cell regulation by altering gene regulation. Also, many metals are potent co-carcinogens, which means they have a synergistic impact when combined with other cancer-causing chemicals. Therefore, metals' potential to trigger changes at the cellular level may be far greater than previously imagined. Current research findings about the sensor-based detection processes of carcinogenic metals in diverse matrices are outlined in this study. Particular attention has been given to metals considered toxic and subsequently designated as Group 1 carcinogens by the IARC, for which most of the data on their genotoxic effects is available. Cancer development is understood to be a three-step process that includes initiation, promotion, and progression. Most of the time, it is unknown if these metal complexes work either as a tumour promoter or an initiator, or both (Huang et al., 2004).

A biosensor is popularly described as an analytical tool consisting of a biological material immobilized in close proximity to a compatible transducer which translates a biochemical signal into a quantifiable optical or electrical signal (Chandra and Suman, 2021; Gronow, 1984; Mahato et al., 2016;

 doi:10.20944/preprints202401.1006.v1

Purohit et al., 2020b). Biosensors are used in almost every field (Azad et al., 2022; Mahato et al., 2018b), and one such is detecting health-deteriorating carcinogenic metals. According to reports, most heavy metals can potentially cause cancer and are carcinogenic. They are systemic toxicants harmful to cell organelles like mitochondria, nucleus, and cell membrane (Karthik et al., 2022). Heavy metal contamination in wastewater and drinking water is relatively high in developing nations like India, Ethiopia, and China (Huang et al., 2019). The primary exposure comes from man-made activities, with a significant chunk of contamination arising from activities such as mineral mining and smelting with metals and their different compounds in home, industrial, and agricultural settings. The interaction of heavy metal ions with DNA and other nucleic acids can lead to damage in DNA and conformational changes that affect cell cycle regulation and apoptosis (Fu and Xi, 2020). Enough efforts have been made to establish delicate and specific methods for recognizing hazardous heavy metal ions. To detect carcinogenic metal ions, various recognition materials, such as biological/synthetic, organic/inorganic, optical, laser, or combination materials, have been used (Alhadrami, 2018). And these materials, as mentioned here, are regarded as Heavy Metal Recognition Materials. Some of them can be biological receptors, electrochemical receptors, chemical receptors, alloys, ionophores, fluorophores, or carbon nanotubes. Several biosensors based on DNAzymes/DNA particles have also been developed (Zhou et al., 2020). Many enzymes have been used to analyze heavy metal ions based on the activation or inhibition of their enzymatic activity. Enzyme activation occurs when heavy metals act as cofactors for metalloproteins, essential to enzyme structure and function. Several non-enzymatic proteins have also been used in biosensor development, ranging from naturally occurring metal-binding proteins to various synthetically designed proteins built to bind certain metal ions (Verma and Singh, 2005). For the biomonitoring of setups contaminated by heavy metals, proteins conferring resistance to metals or participating in regulatory mechanisms and synthesized by genetically modified organisms have been used to detect cadmium and lead (He et al., 2021). Apart from these, immunoassay techniques have also been reported. They have become a popular alternative for detecting heavy metal ions due to their significant advantages over traditional detection techniques. Appropriate antibodies can be generated to enhance the selectivity, sensitivity, species specificity, and theoretical applicability to any contaminant (Verma and Singh, 2005). All these recent examples are types of biological receptors. Nowadays, reports of detecting heavy metals utilizing artificial receptors, such as ionophores, are also prevalent (Zhou et al., 2016). Similarly, fluorescent molecules are also utilized for the detection of carcinogenic metals (Sannigrahi et al., 2019). One such novel technique is thessDNA multi-walled carbon nanotube (MWCNT) integrated fluorescent system for the detection of heavy metal ions (Karthik et al., 2022). It combines the properties of both ionophores and fluorophores. An advanced method of sensing carcinogenic metal ions includes the lab-on-chip method. Within a micro total analysis setup, lab-on-chip systems can perform a variety of chemical, biological, and related procedures and thereby detect heavy metals. These chips are fabricated using glass, silicon, polydimethylsiloxane (PDMS), polymethylmethacrylate (PMMA), and polycarbonate polymers (Lu et al., 2018; Zhang et al., 2020). Even a minute amount of toxic metal concentration, ranging from picomolars to micromolars, can be detected using this combination.

For the immobilization of the recognition material on the transducer's surface, biomaterial functionality is essential. It is also crucial to ensure the receptor cell's accessibility to analytes and the closeness between the bioreceptor and the transducer. For every sensor used for the detection of carcinogenic metal, the sensor's immobilization method is significant, which is determined on the basis of the physicochemical parameters of the analyte, the type of sensing device utilized, and the operating conditions(Purohit et al., 2020a). In this review article, the detection of five prominent carcinogenic metals has been discussed in detail: As, Cd, Be, Ni, and Cr, along with their mechanisms of causing cancer. The biosensors developed for their detection have been discussed thoroughly, and future prospects have also been discussed.

Preprints (www.preprints.org) | NOT PEER-REVIEWED | Posted: 15 January 2024 doi:10.20944/preprints202401.1006.v1

Biosensors for the detection of arsenic

As is a long-lasting poisonous heavy metal that seriously endangers the environment and public health by being present in water. It is a fact that As pollution in the environment has been a global issue owing to its toxicity to both humans and microorganisms. As per the World Health Organization (WHO), the permissible quantity of As should be less than 10 ppb in drinking water, but if it is greater than that, it can cause skin, lung, heart, and bladder cancer and renal problems in the long run (Online et al., 2018; Rahman et al., 2016). Taxonomically diverse and metabolically adaptive microorganisms are involved in the redox conversion of As and can use it to produce energy by oxidation (Hughes et al., 2011). The oxidation state of this metal ranges from 0 in the elemental state to +2 in As_4S_4, +3 in AsH_3, and +4 in H_3AsO_4. In the aqueous medium, As is mainly found as the in form of As^{5+} (pentavalent arsenate) and As^{3+} (oxyanions of trivalent arsenite). The presence of As^{3+} is 60 times more hazardous than As^{5+} (as H_3AsO_4), if present in potable water.

As itself is not mutagenic, however, it has been known to have several damaging effects on DNA, such as amplifying DNA damage caused by other substances, inhibiting sister chromatid exchange, gene duplication, and DNA repair. Its intake via contaminated food or water leads to its absorption in the digestive system. Trivalent arsenic (As^{3+}) enters the cell through aquaglyceroporin channels, whereas pentavalent arsenic (As^{5+}) enters cells through membrane transporters such as the phosphate transporter. The trivalent form of As is more membrane-permeable than pentavalent ones, and its uptake is greatly influenced by cell type and oxidation state. Arsenate reductase is an enzyme that can either be expelled from cells or sequestered in intracellular compartments, converting As^{5+} to As^{3+}. The process of converting As from its inorganic to the organic state involves methylation. By methylating arsenite, first to monomethylarsonous acid (MMA) and then to dimethylarsonous acid (DMA), the arsenic-3-methyl transferase enzyme (As_3MT) uses s-adenosyl-l-methionine (SAM) as the methyl-donating cofactor. Glutathione-s-transferase omega (GSTO) is the enzyme that catalyzes the conversion of MMA_5 to MMA_3. The liver is known to absorb the inorganic arsenicals, convert them to MMA and DMA, and then excrete pentavalent methylated arsenic into the urine. Additionally, it has been claimed that arsenic can activate signal transduction pathways and encourage the production of reactive oxygen species (ROS). Similar to many other traditional carcinogens, it stimulates cell proliferation. An understanding of the process underlying As carcinogenicity can be gained from how arsenic affects cell proliferation. According to research done by the Agency for Toxic Substances and Disease Registry (ATSDR) (2013), even after stopping exposure to As, 40 and 60 percent of the toxin may remain in the body's tissues, such as skin, hair, nails, and muscle, with smaller quantities remaining in the teeth and bones. This continues to contribute to the toxicity and carcinogenicity of As (Bustaffa et al., 2014).

As a result, it is essential to identify As levels in the natural resources, the environment, and the human body. This is done using several analytical techniques, but the most advanced and sensitive technique is sensing. Some of the biosensing techniques have been discussed below.

Electrochemical biosensors are the most sought-after, rapid, and sensitive (Mahato et al., 2018a). For instance, Núñez et al. mounted the bacteria *Alcaligenis faecalis* on a screen-printed carbon electrode (SPCE) augmented with gold nanoparticles (AuNPs-SPCE) as an electrochemical biosensor for As^{3+} ion detection (Núñez et al., 2021). Without a redox mediator, the bacteria were crosslinked with glutaraldehyde over AuNPs-SPCE. By catalytically converting As^{3+} to As^{5+} upon activation, the bacterial enzyme arsenite oxidase created an analytical signal that enabled the detection of As^{3+} ions. The limit of detection (LOD) was obtained as 6.61 μmol L^{-1} (R = 0.9975) at 700 mV (pH 12) in the analytical application. After reduction, the As concentrations in river water samples were assessed using the electrode AF/AuNPs-SPCE. Similarly, another electrochemical-based aptamer biosensor for As detection has also been developed by Yadav et al. They modified glassy carbon electrodes (GCE) using silver and gold alloy nanoparticles (Ag-Au alloy NPs), which were eventually loaded with an aptamer (Yadav et al., 2020). The electrode contained apta-deep trapped Ag-Au alloy nanoparticles (NPs), and the detection was carried out using differential pulse voltammetry (DPV) and cyclic voltammetry (CV) methods. Voltammetry results showed that the electrochemical process in which the As^{3+} ions were collected underwent a significant increase in current. The NPs' electrocatalytic properties

Preprints (www.preprints.org) | NOT PEER-REVIEWED | Posted: 15 January 2024 doi:10.20944/preprints202401.1006.v1

led to an increase in current. For As^{3+} concentration, the activity curve was investigated to be linear with values between 0.01 µg/L to 10 µg/L and the LOD value to be 0.003×10^{-3} µg/L. Another advanced electrochemical biosensor for the immobilization-free detection of As^{5+} was developed by Yang L et al. CeO_2-DNA was used as a nanoprobe based on the competitive coordination effect (Yang et al., 2020). CeO_2 NP was created, followed by the adsorption of ssDNA over CeO_2, thus forming a bio-conjugate where the ssDNA took up the As^{5+} via a coordination bond. More notably, this immobilization-free electrochemical method avoided the complex modification and time consumption, displaying exceptional simplicity, speed, and efficiency compared to the conventional As^{5+} electrochemical assays. The fabrication and working of this biosensor have been illustrated in **Figure 1A**.

Apart from the electrochemical biosensors, luminescent sensors have also been developed. Dieudonné et al. developed a whole-cell biosensor using magnetotactic bacteria that show intrinsic magnetism (Dieudonné et al. 2020). Initially, in the genomes of two strains of magnetotactic bacteria, *Magnetospirillum gryphiswaldense (MSR-1)* and *Magnetospirillum magneticum (AMB-1)*, As-inducible promoters were found. With a LOD value of 0.5 µM for arsenite, a biosensor was created by transcriptional fusion between the luxCDABE operon of bacteria and the As-inducible promoters. It produced an element-specific response in 30 minutes. Post magnetic concentration, the biosensor's sensitivity increased by a factor of 50, bringing it to 10 nM. That was more than an order of magnitude below the 0.13 M upper limit for As in drinking water. Upon freeze-drying the magnetic bacteria, the biosensor resulted in successful preservation. In another recent successful work on photoluminescent biosensors by Dwivedi A et al., Eu:Y_2O_3 nanophosphor (EYN) and Eu:Y_2O_3-poly vinyl alcohol (PVA) fluorescent films (EYF) were synthesized to detect As^{3+} (Dwivedi et al., 2022). With an arsenate solution, the EYF probe exhibited a rapid fluorescence quenching reaction. The LOD for arsenate detection was estimated to be 57.4 ng/L (0.0574 ppb), with a linear detection range of 0-100 µg/L. The fabrication of a biosensor has been shown in **Figure 1B**. The probe also exhibited remarkable durability and required no acid medium or enzyme.

In recent years, various novel biosensors integrated with microfluidic devices have also been developed for detecting and quantifying arsenic. One such example is a paper-based microfluidic sensor device that was modified with silver nanoparticles for the colorimetric naked-eye detection of As^{3+} (Saadati et al., 2022). The fabrication of the biosensor has been demonstrated in **Figure 1C.** The oxidation-reduction reaction between silver nitrate and As^{3+} and further deposition on Ag nanoprisms (NPrs) changed their morphology. Subsequently, a change in the color of the nanoparticle from blue to purple was observed. Based on this phenomenon, a method for As^{3+} naked-eye detection was developed. The developed device provided a quick visual approach with As^{3+} analysis capability ranging from 0.0005 to 1 ppm, with 0.0005 ppm as the lower limit of quantification (LOQ).

Some additional examples of biosensors reported to detect As have been mentioned in **Table 1,** where the sensing molecule, fabrication strategy, detection method, linear dynamic range (LDR), LOD, and real sample data have been mentioned precisely.

Preprints (www.preprints.org) | NOT PEER-REVIEWED | Posted: 15 January 2024 doi:10.20944/preprints202401.1006.v1

Table 1. List of biosensors for detection of arsenic (NR-Not reported).

S.No.	Sensing molecule	Detection method	Fabrication strategy	Linear dynamic range (LDR)	Limit of detection (LOD)	Real sample	References
1	Arsenic	CV, Hydrodynamic amperometry	GCE modified with cobalt oxide nanoparticles	NR	11 nM	Aqueous solution	(Salimi et al., 2008)
2	Arsenic	CV, ASV	Metallothionein was adsorbed on a paper chip placed on a SPCE	5 ppb-1000 ppb	13 ppb	Water	(Irvine et al., 2017)
3	Arsenic	CV	Graphene oxide nanosheets based electrochemical biosensor using l-leucine as biorecognition element	5 ppm-50 ppm	0.5 ppm	River, Underground water	(Kumar et al., 2016)
4	Arsenic	SWV	GCE modified with bi-nanoparticle,CNP and AuNPsand conjugated with aptamer	0.5 ppb-100 ppb	0.092 ppb	Water	(Mushiana et al., 2019)
5	Arsenic	EIS	Arsenic-specific aptamer fabricated on gold electrode	0.05 ppm-10 ppm	0.8 µM	NR	(Vega-Figueroa et al., 2018)
6	Arsenic	CV, EIS, DPV	PB-GO nanocomposites assembled on ssDNA-modified gold electrode	0.2 ppb-500 ppb	0.058 ppb	Tap water, river water, lake water	(Wen et al., 2018)
7	Arsenic	CV, LSASV	SPCE fabricated with silica NPs	5 µg/L-30 µg/L	6.2 µg/L	River water, Tap water	(Ismail et al., 2020)
8	Arsenic	Optical (liquid crystal)	CTAB was employed to induce homeotropic orientation of the liquid crystal, and Ars 3 aptamer was used as molecular recognition element	0.02 µM-1 µM	50 nM	Tap water	(Nguyen and Jang, 2020)

 doi:10.20944/preprints202401.1006.v1

9	Arsenic	Fluorescence sensor	Use of a label-free fluorescent detection platform with a molecular triple helix switch as the detection element	10 ng/L-10 mg/L	5 ng/L	Water	(Pan et al., 2018)
10	Arsenic	Fluorescence biosensor	MoS_2 nanosheets (quencher) prepared by Co-precipitation, FAM labeled Ars 3 aptamer used as a signal reporter	0 nM-8 nM	18 nM	Tap water, lake water	(Ravikumar et al., 2018)
11	Arsenic	Fluorescence biosensor	Label-free streptavidin and aptamer-coated silica nanoparticles based on target-induced conformational changes of biotin and complementary aptamer strands	2 nM -500 nM	0.45 nM	Tap water, serum sample	(Taghdisi et al., 2018)

List of abbreviations: CV- Cyclic Voltammetry, GCE – Glassy Carbon Electrode, ASV- Adsorptive Stripping Voltammetry, SWV- Square Wave Voltammetry, EIS – Electrochemical Impedance Spectroscopy, DPV- Differential Pulse Voltammetry, LSASV – Linear Sweep Adsorptive Stripping Voltammetry, AuNPs- Gold Nanoparticles, CNP- Carbon Nanoparticle, PB- Prussian Blue, GO- Graphene Oxide, CTAB- Cetyltrimethyl Ammonium Bromide, FAM- Fluorescein amidites.

Preprints (www.preprints.org) | NOT PEER-REVIEWED | Posted: 15 January 2024 doi:10.20944/preprints202401.1006.v1

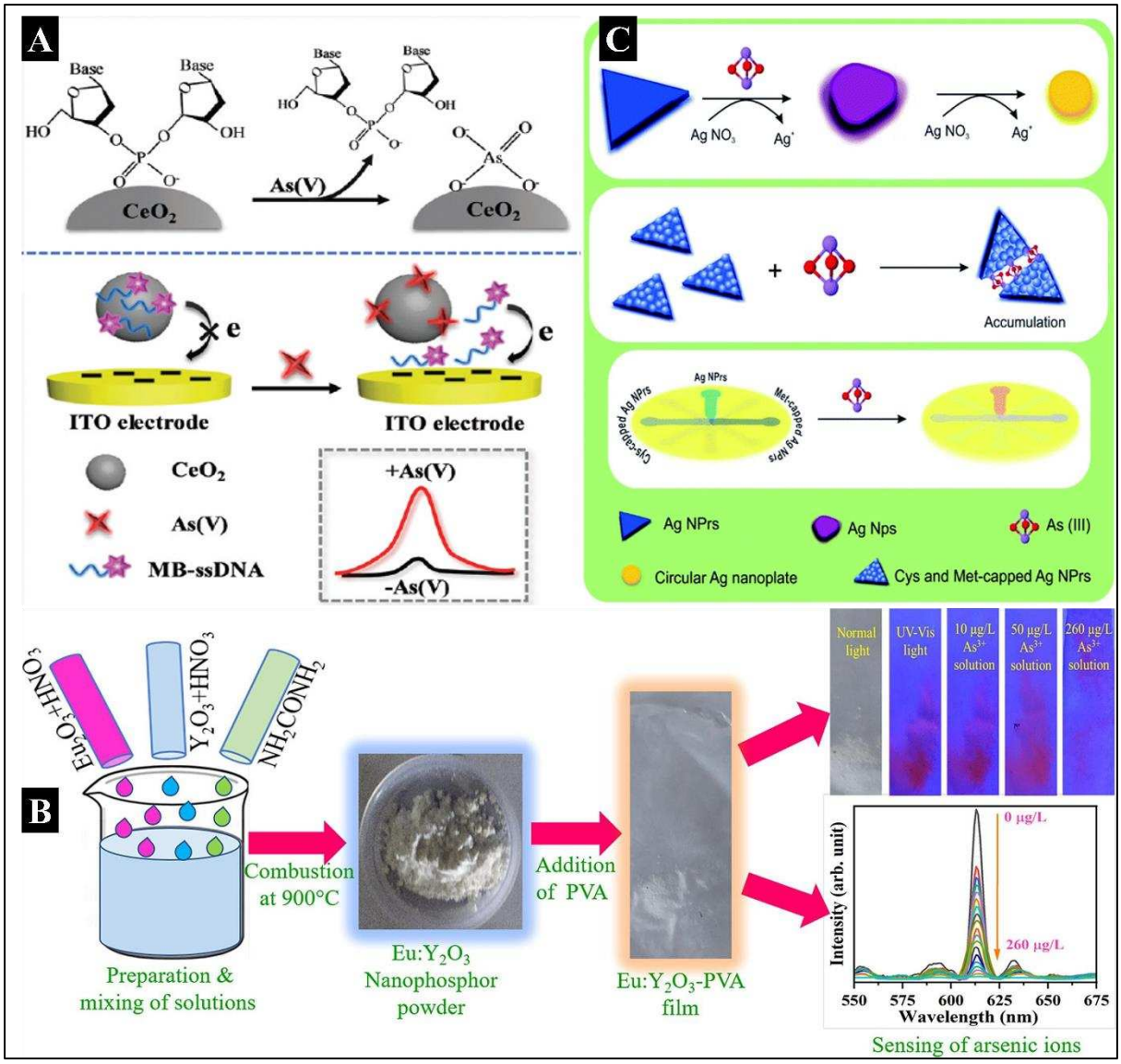

Figure 1. A) Fabrication of an electrochemical biosensor (immobilization-free) for As^{5+} detection using nanoprobes (adapted with permission from (Yang et al., 2020); B) Fabrication of biosensor for detection of As^{3+} using Eu:Y_2O_3 -nanophosphor (EYN) and EYN dispersed-PVA fluorescent film (EYF) (adapted with permission from (Dwivedi et al., 2022);C) Fabrication of colorimetric biosensor based on Ag NPs for naked eye As^{3+} detection (adapted with permission from (Saadati et al., 2022).

Biosensors for the detection of beryllium

Be is not considered a heavy metal because of its low density and exhibits some unique properties, such as a high melting point and greater stiffness**.** Along with such properties, Be is considered one of the most toxic elements that can cause several types of cancer and chronic beryllium disease (CBD) (Kreiss et al., 1997). Its toxicity happens mainly due to contamination of water and air in the Be^{2+} form. It is found in trace amounts in natural and wastewater and accumulates in the skin and soft tissues. Be^{2+} is a competing ion for Mg^{2+} at biological binding sites like the phosphate groups of nucleotides and nucleic acids because it has the same charge as Mg^{2+}, but Be does not take part in redox processes. It leads to the uncontrolled growth of cells, making it a major contributor to cancer. It promotes mitogenic signaling pathways just as other metal compounds which are carcinogenic. Additionally, Be^{2+} increases the expression of cellular proto-oncogenes *in vitro* (Beyersmann and Hartwig, 2008).

Owing to its contribution to cancer, its detection is very crucial. Traditionally, it was determined by electrothermal-atomic emission spectrometry, atomic absorption spectrometry, liquid

Preprints (www.preprints.org) | NOT PEER-REVIEWED | Posted: 15 January 2024 doi:10.20944/preprints202401.1006.v1

chromatography, chelate gas chromatography, inductively coupled plasma mass spectrophotometry, and fluorospectrophotometry (Wang et al. 2006; Li et al. 2015a). These approaches, however, either need costly equipment, labor-intensive sample processing or lack appropriate sensitivity and selectivity. Additionally, interfering chemicals in samples make identification more difficult. Therefore, it is essential to have susceptible and specific detection methods to identify low-traced Be in water and food samples. Biosensing can be an effective way to detect and quantify Be^{2+} ions in water (Chandra et al., 2013). Some of the new biosensors designed have been discussed explicitly here.

To determine Be^{2+} in water and tetrahydrofuran (THF), a new multichannel sensor based on two asymmetrical phthalocyanine molecules was created by Yavuz O. et al. The structure of the biosensor was studied using single crystal X-ray diffraction (XRD) and spectroscopic methods such as ^{1}H-NMR, ^{13}C-Nuclear Magnetic Resonance (NMR), UV-Vis, infrared spectroscopy (IR), matrix assisted laser desorption/ionization time of flight mass spectroscopy (MALDI-TOF-MS), and steady-state fluorescence (Yavuz et al., 2021) . The LOD value was calculated to be 2.9 ppb, which was relatively lower than the WHO's threshold limit of 4 ppb in an aqueous solution. The sensor fabrication has been illustrated in **Figure 2A.** Compared to other reported sensors in the literature, these sensors can be categorized as fast sensors with a super quick response time between 0.6 - 0.7 s, respectively. In this sensor, a small amount of interference from Co^{2+} was observed. Also, Qin J et al. developed a unique type of biosensor using photonic hydrogel (Qin et al., 2018). **Figure 2B** shows the fabrication of a hydrogel sensor. The smallest cavity-containing crown ether molecules were functionalized in responsive photonic hydrogels intended to detect the minute level of Be^{2+} ions. The detection was done in a seawater system by a volume-induced structural color change of colloidal photonic crystals (CPCs) (non-close-packed) immobilized in the hydrogels. Cryotropic gelation was used to embed the CPCs in suspension within the scaffold PVA hydrogel. It was followed by a photochemical reaction on top of the PVA layer to covalently bind the ion-recognition functional groups, forming an additional polyacrylamide hydrogel. This two-step adaptable polymerization method was used to create the intelligent hydrogel sensing material. The hydrogel that was left post removal of the PVA scaffold revealed bright structural color due to photonic crystal diffraction in the visible spectrum and the strong and precise binding of the grafted benzo-9-crown-3 (B9C3) with Be^{2+} ions in solution. The hydrogel sensor can quantitatively detect Be^{2+} ions in seawater and achieve an LOD of 10^{-11} M. This design and construction have been proven for the detection of Be^{2+} as an inexpensive and efficient sensor for *in-situ* monitoring of harmful ions in seawater. In another type of biosensor, Peng et al. have developed a microcantilever sensor based on polymer brushes functionalized with B9C3 for the selective and sensitive detection of Be^{2+} ions in aqueous medium (Peng et al., 2017). The LOD for the Be^{2+} ion was 10^{-10} M, and the cantilevers demonstrated great sensitivity and selectivity. The microcantilever modified with functionalized B9C3 polymer brushes has the potential to be a trustworthy and durable sensor for Be^{2+} detection, as proven by the quick response time (3 min) and the cantilevers' complete reusability. The sensitivity of the modified microcantilever Be^{2+} sensor was better than that of laboratory techniques such as spectroscopy and atomic absorption technologies. However, more enhancement of the microcantilevers' surface properties is possible. In addition to the above, a Be^{2+} optode optical sensor was crafted by Beiraghi A et al. In this, the membrane was prepared by adding 1,8-dihydroxy anthrone and sodium tetraphenyl borate (NaTPB) to a plasticized poly-vinyl chloride membrane using ortho-nitrophenyl octyl ether (o-NPOE) as a plasticizer (Beiraghi et al., 2011). When exposed to Be^{2+} ions at pH 10.5, the detecting membrane's color changed rapidly from orange to red. In optimized circumstances, the developed sensor displayed a LDR of 0.1-5 g L^{-1} and an LOD of 0.03 g L^{-1}. The probe's selectivity was tested for various anions and cations. Ethylenediaminetetraacetic acid (EDTA) can be a valuable tool for quantifying the amount of Beas the sensor was highly selective in the presence of this masking agent. The created sensor, which used a PVC membrane in conjunction with spectrophotometry, is an accurate, economical, highly sensitive, and highly selective tool for the measurement of Be^{2+} ions. By utilizing EDTA as a masking agent for various metal ions, the technique might be made more selective.

 doi:10.20944/preprints202401.1006.v1

Li J et al. created an electrochemical sensor for the detection of Be^{2+} based on a novel molecularly imprinted polymer (MIP)-electrochemiluminescence (ECL) (Li et al., 2015b). The template molecule was chosen as the Be^{2+} and 4-(2-pyridylazo)-resorcinol combination for MIP. The fabrication and mechanism of the biosensor detection have been illustrated in **Figure 2C**. The complex molecule could escape from the MIP and be uniquely recognized by the formed cavities. To convey the probe molecules required to produce a sound-responsive signal, the produced cavities act as a tunnel. Thus, the Be^{2+} concentration was indirectly determined based on the strength of the signal, which was proportional to the complex molecule's concentration in the sample solution. The investigations revealed that, with a LOD of 2.35×10^{-11} mol/L, the ECL's intensity demonstrated linearity in the 7×10^{-11} - 8.0×10^{-9} mol/L range.

Apart from all the discussed techniques, only a few more biosensors are reported for Be in the literature and presented in **Table 2,** where the sensing molecule, fabrication strategy, detection method, LDR, LOD, and real sample data have been described precisely for reference.

Preprints (www.preprints.org) | NOT PEER-REVIEWED | Posted: 15 January 2024 doi:10.20944/preprints202401.1006.v1

Table 2. List of biosensors for detection of Beryllium (NR-Not reported).

S.No.	Sensing molecule	Fabrication strategy	Detection method	Linear Detection Range (LDR)	Limit of Detection (LOD)	Real Sample	Reference
1	Beryllium	CV, EIS	Beryllium-PAR complex used as a template for MIP, MIP-electrodes immersed in a sample with PAR to detect Be (II)	Bottled water, Rice sample	7×10^{-11}-8×10^{-9} M	2.35×10^{-11} mol/L	(Li et al., 2015b)
2	Beryllium	ASV	Adsorptive accumulation of Be-arsenazo-I complex at mercury film-coated carbon-fiber electrode	Sea water	10-60 µg/L	0.25 µg/L	(Wang et al., 2006)
4	Beryllium	Optical (florescence)	To detect Be(II) in THF and aqueous fluids, a multichannel sensor based on unsymmetrical phthalocyanines P—A3BZnPc (1) and its water-soluble version Q—A3BZnPc (2) was developed	Tap water	4-199 ppb for P—A3BZnPc (1) 16-256 ppb for Q—A3BZnPc (2)	2.9 ppb P—A3BZnPc (1) 17 ppb for A3BZnPc (2)	(Yavuz et al., 2021)
5	Beryllium	Optical (fluorescence)	A second ion recognition functional group was covalently bonded to additional polyacrylamide	Sea water	NR	10^{-11} M	(Qin et al., 2018)

 doi:10.20944/preprints202401.1006.v1

			hydrogen over the scaffold-containing PVA hydrogel to detect the beryllium ion				
6	Beryllium	Optical (Absorption)	The 1,8-dihydroxy anthrone and sodium tetraphenylborate (NaTPB) were added to a plasticized poly vinyl chloride membrane that contained ortho-nitrophenyl octyl ether (o-NPOE) as a plasticizer to create an optode membrane	Tap water, mineral water, river water	0.1-5 μg/ml	0.03 μg/ml	(Beiraghi et al., 2011)
7	Beryllium	Potentiometric	The creation of a PVC-based beryllium ion-selective electrode used -4-bromo-1-methoxybenzene as an ionophore	Tap water	3×10^{-6}-7×10^{-2} M	2×10^{-6} M	(Soleymanpour et al., 2006)

List of abbreviations: CV- Cyclic Voltammetry, PAR- 4-(2-Pyridylazo)-resorcinol, MIP – Molecularly Imprinted Polymer, EIS – Electrochemical Impedance Spectroscopy, ASV- Adsorptive Stripping Voltammetry, PVA- Poly Vinyl Alcohol, THF- Tetrahydrofuran, PVC- PolyVinyl Chloride.

Preprints (www.preprints.org) | NOT PEER-REVIEWED | Posted: 15 January 2024 doi:10.20944/preprints202401.1006.v1

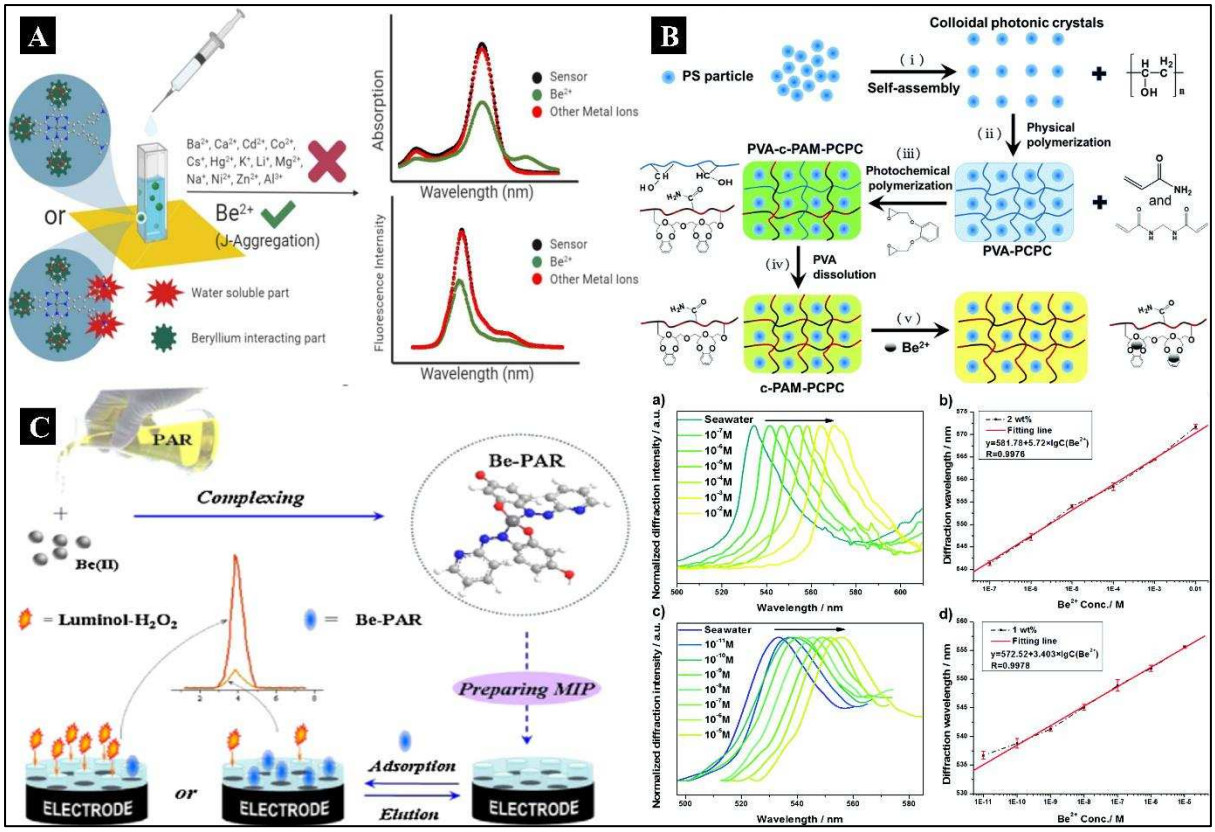

Figure 2. A) Sensitivity and selectivity of developed sensor based on two types of Phthalocyanines : P—A3BZnPc & Q—A3BZnPc for Be^{2+} detection in aqueous environments (adapted with permission from (Yavuz et al., 2021); B) Fabrication of the functional hydrogel sensor for Be^{2+} detection and diffraction responses of functionalized hydrogels containing benzo-9-crown-3 to seawater Be^{2+} ion concentrations (adapted with permission from (Qin et al., 2018); C) Mechanism for the MIP sensor's measurement and recognition for Be^{2+} detection (adapted with permission from (Li et al., 2015b) .

Biosensors for the detection of cadmium

Cd is a non-essential heavy metal for human or animal nutrition and is extremely harmful to both species, even at very minute concentrations. It is a highly toxic heavy metal that enters the environment through several anthropogenic factors. These include mining, refining of non-ferrous metals, discarded rechargeable alkaline batteries (such as Ni-Cd batteries), tobacco smoking, smelting, electroplating, the usage of phosphate fertilizers, and the burning of fossil fuels (Elcin and Öktem, 2020). Huge accumulations of this metal can be found in molluscs and crustaceans, whereas trace amounts can be found in vegetables, grains, and starchy rhizomes. Both humans and animals can absorb it through breathing and digestion. It is present as highly toxic Cd^{2+} ions in the soil, water, and agriproducts (Zeng et al., 2019). As per the IARC 2012, Cd and its compounds are classified under Group 1 human carcinogens as they induce carcinogenesis in the pancreatic, pituitary, hepatic, adrenal, and hematopoietic systems due to prolonged exposure (Elcin and Öktem, 2020). Itai-itai disease, a painful and disabling bone disease, is also caused when calcium is replaced by Cd in the bones (Aoshima, 2016). This leads to osteoporosis, renal tubular failure, and hypercalciuria. Cd inhalation can cause chronic obstructive pulmonary disease. Because they share characteristic properties with zinc, such as the oxidation state, this metal ion disrupts zinc metabolism. It also interacts with iron to lower haemoglobin levels, which results in anaemia (Chakraborty et al. 2013; Jaishankar et al. 2014).

The mechanism of Cd toxicity is different from others. Depending on the route of entry, different amounts of Cd are absorbed in the body after exposure. Approximately 3–10% of the Cd that is consumed is absorbed through the digestive tract, compared to 50% of the Cd that is breathed. After absorption, Cd is quickly carried by the blood to various organs, where it is believed to have a half-life

Preprints (www.preprints.org) | NOT PEER-REVIEWED | Posted: 15 January 2024 doi:10.20944/preprints202401.1006.v1

of 15-20 years in humans. A tiny protein called metallothionein (MT), which has a strong affinity for the metal Cd, is largely responsible for the wide variations in the quantity of Cd retained in different organs. The majority of the Cd is deposited in the liver and kidney, which have high MT concentrations. Other organs that can store Cd include the testis, spleen, heart, lungs, thymus, salivary glands, epididymis, and prostate (Beyersmann and Hartwig, 2008). Therefore, it is crucial to continuously monitor environmental Cd levels to prevent its buildup in the food chain and environment. High selectivity and sensitivity are efficient ways to assess the worth of a monitoring method (Chen et al., 2016). Atomic absorption spectroscopy (AAS) (Karimi et al., 2014), inductively coupled plasma mass spectrometry (ICP-MS) (O'Sullivan et al. 2013), and atomic fluorescence spectrometry (AFS) (Zhang et al., 2016) are examples of conventional detection techniques. These procedures are efficient at quantifying Cd^{2+} but are also time-consuming, expensive, and difficult because of the instrumentation required. To cater for these problems, various biosensors with electrochemical, optical, and fluorescent readouts have recently been developed to monitor Cd^{2+} (Chandra et al., 2015) .

Recently, a bacterial biosensor has been developed that uses a visual pigment as the output signal to respond only to hazardous Cd^{2+} (Hui et al., 2022). A metabolically modified bacteria was used to create the violacein pigment (a blue-purple pigment) that reacts with toxic Cd^{2+}. After 1.5 hours of Cd^{2+} treatment, signals resulting from the pigment's excellent stability were observed at 578 nm wavelength and measured. A step by step protocol of biosensor fabrication has been given in **Figure 3A**. Compared to other heavy metals, including Zn^{2+}, Pb^{2+}, and Hg^{2+}, this novel biosensor responded to Cd^{2+} far more robustly. The LOD value was detected to be as low as 0.049 μM. This Cd^{2+} -induced violacein production offers a quick-responding, inexpensive, and low-equipment biosensor that may be utilized to determine the eco-toxicology of heavy metals. Similarly, another bacterial biosensor was developed to measure extractable and total Cd in real environmental samples with high sensitivity, selectivity, and cost-effectiveness towards Cd^{2+} by Cai Y et al. The Cd-responsive biosensor was created through directed evolution using the reporting element, GFP and the regulatory element, CadR (Cai et al., 2022). A schematic of biosensor fabrication is shown in **Figure 3B**. Through the use of continuous fluorescence-activated cell sorting (FACS) and polymerase chain reaction (PCR), mutant libraries of biosensors were created, among which the bacteria variant epCadR5 showed improved performance. According to the fluorescence intensity measurement results, the evolved Cd-responsive bacterial biosensor had a high specificity and sensitivity for detecting trace levels of Cd. The recorded LOD value of 0.45 μg/L was 6.8 times more sensitive to Cd than the wild-type biosensor. ICP-MS and the Cd readings from epCadR5 bacteria were shown to be equivalent by quantitative analysis. These findings imply that a wide range of Cd-contaminated water and soil detection applications might be possible with the developed biosensor. This biosensor has higher interference-fighting abilities than the previous generations of Cd-responsive bacterial biosensors, which could not meet the demands of practical detection.

In addition to whole-cell biosensors, DNA-based electrochemical biosensors are also widely used nowadays (Sreekanth SP et al.). First, the GCE was fabricated with MWCNT, and then it was immobilized with dsDNA to serve as the working electrode for the detection of Cd^{2+}(Sreekanth et al., 2021). The indicator dye, EG, adhered to ssDNA preferentially, and the reduction peak current was smaller for dsDNA. When the indicator dye (EG) bonded to ssDNA instead of dsDNA, the reduction peak current was enhanced. First, the Cd^{2+} unzipped the dsDNA to ssDNA following their binding, and the EG molecules then attached to the ssDNA, increasing the reduced peak current, which varied depending on the concentration of Cd^{2+}. The stepwise fabrication is shown in **Figure 3C**. The LOD for this method was 2 nM, which was lower than the WHO-permitted level for human exposure, and it produced an LDR of 2 nM-10.0 nM with 5 nA nM^{-1} sensitivity. In another study by Xue Y et al., an aptamer-based biosensor for Cd^{2+} detection was developed using dual polarization interferometry (DPI), which was label-free and regenerable (Xue et al., 2020). The fabrication and detection of Cd^{2+} at high and low concentrations have been depicted in **Figure 3D.** This aptasensor investigated the real-time interaction between Cd^{2+} and its aptamer. An interaction mechanism and aptamer conformation

 doi:10.20944/preprints202401.1006.v1

dependent on Cd^{2+} concentration was proposed based on the measured mass, thickness, and density. At low Cd^{2+} concentrations, Cd^{2+} interactions with phosphate groups on aptamers resulted in a stretched ssDNA and a few vertical hairpins. The developed aptasensor showed remarkable sensitivity and specificity for Cd^{2+} detection and was noticeably more sensitive than the 5.0 µg/L threshold imposed by the US Environmental Protection Agency (EPA) with a LOD value of 0.61 µg/L. The biosensor also had excellent regeneration capability and could be used again without changing the response signal noticeably. Interestingly, a label-free electrochemical biosensor has been developed for the detection of Cd^{2+} by Li Y et al. The isothermal titration calorimetric method was initially used to screen out the Cd^{2+} aptamer (issAP08-Cd^{2+}), which revealed that the equilibrium dissociation constant (K_D) of Cd^{2+} binding with issAP08-Cd^{2+} was 2.9 µM. After that, thiol was used to modify the ssDNA (issAP08-Cd^{2+}) having 25 nucleotides before assembling it on a gold screen-printed electrode (Li et al., 2019). Following that, the Cd^{2+} solution was dropped on the SPE in order to detect Cd^{2+} using the electrochemical aptasensor. The electrochemical characteristics were identified using CV and DPV, and the LOD value was determined to be 0.05 ng/mL. This result reaffirmed the idea that the electrochemical aptasensor has outstanding selectivity and sensitivity and performs admirably well in applications involving real samples owing to its satisfactory reproducibility and stability outcomes.

Other biosensors which have been reported over time are enlisted in **Table 3,** where sensing molecules, fabrication strategies, detection methods, LDR, LOD, and real sample data have been mentioned precisely for detecting and quantifying Cd^{2+} in water, soil, and food materials.

Preprints (www.preprints.org) | NOT PEER-REVIEWED | Posted: 15 January 2024 doi:10.20944/preprints202401.1006.v1

Table 3. List of biosensors for detection of Cadmium (NR-Not reported).

S.No.	Sensing molecule	Detection method	Fabrication strategy	LDR	LOD	Real Sample	References
1	Cadmium	DPV	CPE modified with dsDNA and brilliant green is used as an indicator molecule	Animal (Rat tissue, chicken tissue)	0.05×10^{-9} mol/L - 1.2×10^{-9} mol/L	0.1×10^{-12} mol/L	(Ruhan et al., 2020)
2	Cadmium	DPV	DNA-based biosensor using ethyl green as DNA hybridization indicator on the surface of CPE	Tap water and sea water	1 pM-1 nM and 10 nM-1 μM	0.3 pM	(Ebrahimi et al., 2018)
3	Cadmium	EIS, SWV	Immobilization of β-GAL on electrochemical transducer by crosslinking with glutaraldehyde and detection was based on inhibition of β-GAL by Cd	River water	2.36–2.36 × 10^{7} μg/L by EIS 2.36 × 10^{-3}–2.94 × 10^{7} μg/L by SWV	6.95 μg/L by EIS 7.61ng/L by SWV	(Fourou et al., 2016)

Preprints (www.preprints.org) | NOT PEER-REVIEWED | Posted: 15 January 2024 doi:10.20944/preprints202401.1006.v1

4	Cadmium	DPV	Cd aptamer functionalized on (AuNPs/CS)-GCE	Tap water	0.001 nM-100 nM	0.04995 pM	(Liu et al., 2017)
5	Cadmium	CV, EIS	Aptamer conjugated reduced Graphene oxide/ graphitic carbon nitride	Tap water, lake water, industrial waste from paper mill	1 nM-1 μM, 1 μM-1 mM	0.337 nM	(Wang et al., 2018)
6	Cadmium	CV, DPV	Fabrication of aptamer on modified gold screen-printed electrode	River Sample, Fish sample	0.1 ng/mL-1000 ng/mL	0.05 ng/mL	(Li et al., 2019)
7	Cadmium	CV	Fabrication of aptamer on Ti-modified Co_3O_4 NPs placed on SPCE	River water, Tap water	0.20 ng/mL -15 ng/mL	0.49 ng/mL	(Liu et al., 2020)
8	Cadmium	DPV	Immobilization of dsDNA on GCE/MWCNT and ethyl green used as an indicator dye	Water	2 nM-10 nM	2 nM	(Sreekanth et al., 2021)
11	Cadmium	Optical biosensor	Liquid crystal biosensor based on Cd^{2+} induced	NR	NR	0.1 nM	(Deng et al., 2015)

Preprints (www.preprints.org) | NOT PEER-REVIEWED | Posted: 15 January 2024 doi:10.20944/preprints202401.1006.v1

			bending of PS oligo (DNA), DNA immobilized on DMOAP/APTES/GA decorated glass slides				
12	Cadmium	DPI (optical biosensor)	To investigate the interaction between cadmium and aptamer, the construction of Label-free and regenerable aptamer-based biosensor by DPI	Tapping water	0.0036 mg/L-7.28 mg/L	0.61 µg/L	(Xue et al., 2020)

List of abbreviations: DPV- Differential Pulse Voltammetry, EIS – Electrochemical Impedance Spectroscopy, SWV- Square Wave Voltammetry, CV- Cyclic Voltammetry, GCE – Glassy Carbon Electrode, DPI- Dual Polarization Interferometry, GCE – Glassy Carbon Electrode, MWCNT- Multi Walled Carbon Nanotubes, DMOAP – N, N-dimethyl-N-octadecyl-3-aminopropyltrimethoxysilyl chloride, APTES – (3-aminopropyl) triethoxysilane, GA-Glutaraldehyde, CPE- Carbon paste electrode.

Preprints (www.preprints.org) | NOT PEER-REVIEWED | Posted: 15 January 2024 doi:10.20944/preprints202401.1006.v1

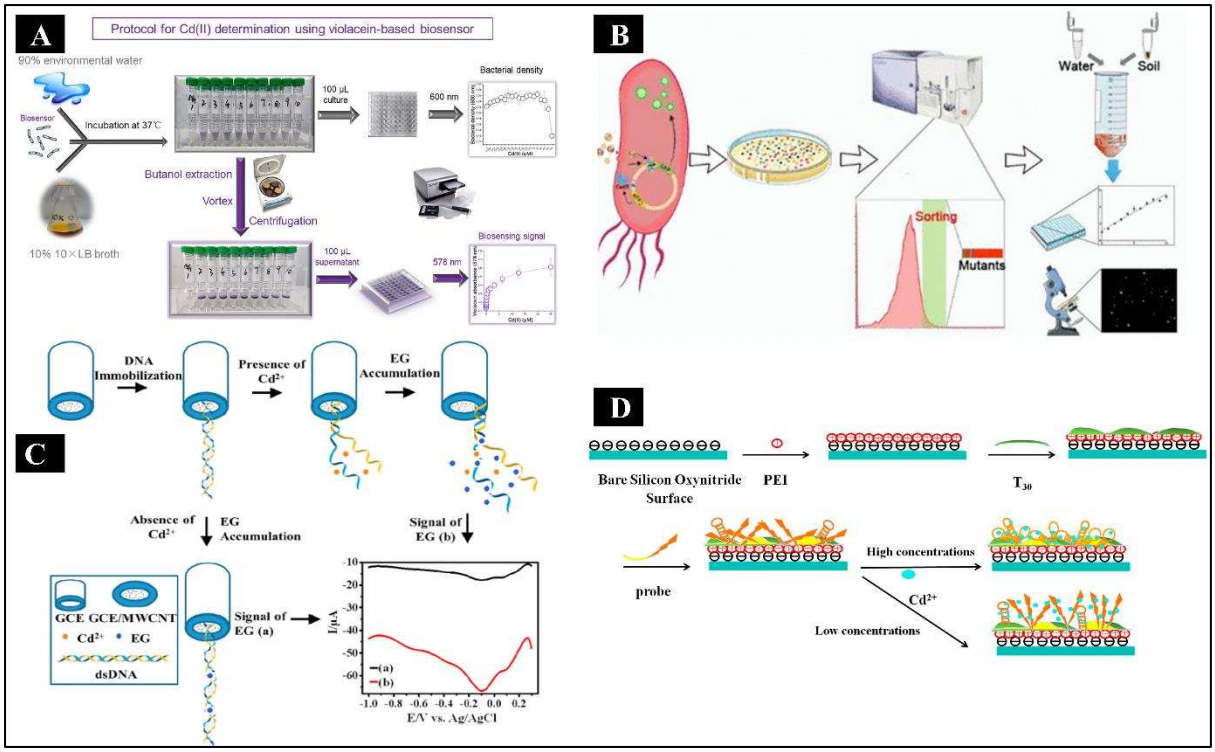

Figure 3. A) Step-by-step protocol for violacein-based bacterial biosensors for Cd^{2+} (adapted with permission from (Hui et al., 2022); B) Schematic of bacterial biosensor formation using regulatory elements (CadR) and reporting elements (GFP) (adapted with permission from (Cai et al., 2022); C) Step-by-step fabrication of nanobiosensors using MWCNTs (adapted with permission from (Sreekanth et al., 2021); D) Schematic of label free and regenerable aptasensor for real-time detection of Cd^{2+} by dual polarization interferometry (DPI) at different concentrations of Cd^{2+}(adapted with permission from (Xue et al., 2020).

Biosensors for the detection of chromium

Cr is another most commonly available element on earth and is ranked 22nd based on its availability. In the environment, it occurs naturally due to the erosion of natural Cr deposits. However, the presence of Cr deposits in the earth's crust depends entirely on regional geochemistry. Cr exists in various oxidation states, including Cr^0, Cr^{2+}, Cr^{3+}, Cr^{4+}, Cr^{5+}, and Cr^{6+}, but the most stable oxidation states are Cr^{3+} and Cr^{6+}, which are commonly found. These Cr compounds are extensively used for various industrial purposes, such as metal finishing and electroplating in the steel industry, alloying, leather tanning, textile dyes, mordants, and industrial catalysts. Due to the varied use of Cr for industrial applications, a large amount of Cr accumulates within the environment (air, water, soil), adversely affecting the ecological cycle. Furthermore, because of its solubility and mobility, Cr^{6+} in the soil can leach into surface water or groundwater. Although the human body needs Cr^{3+} in trace amounts (50-200 mg/day) for its proper functioning, Cr^{6+} is considered highly toxic, about 1000 folds more toxic than Cr^{3+} (even in small amounts) due to its highly oxidizing capacity (Zayed and Terry, 2003). It is responsible for chronic bronchitis, contact dermatitis, liver and kidney damage, ulcers, and even cancer (Sharma et al., 2012). While a threshold of 100 μg L^{-1} total Cr in drinking water is stated safe by the EPA* (web reference 1), WHO recommendations stipulate that the level of Cr^{6+} in groundwater must be less than 50 μg L^{-1} (Biswas et al., 2017; Sayato, 1989).

The entry of Cr into cells and its harmful effects are significantly influenced by its chemistry. In the environment, hexavalent Cr is primarily found as the chromate oxyanion (CrO_4^{2-}). The general sulphate transporters on the cell surface are used by the chromate oxyanion to enter the cell because they share a similar structural makeup with the sulphate oxyanion (SO_4^{2-}). After reduction with ascorbate and biological thiols such as glutathione (GSH) or cysteine amino acid residues, Cr^{6+} begins

Preprints (www.preprints.org) | NOT PEER-REVIEWED | Posted: 15 January 2024 doi:10.20944/preprints202401.1006.v1

to exhibit its harmful effects once within the cell. Cr^{6+} is reduced by GSH to reactive Cr^{5+} using a one-electron reduction, and with either reductant, Cr^{6+} is ultimately converted to Cr^{3+}. In tissue culture systems with very low levels of ascorbate, Cr^{6+} is reduced by GSH to reactive Cr^{5+} using a stepwise two-electron reduction, which typically occurs *in vivo*. This mechanism, particularly when GSH is reduced, can produce high amounts of oxidative stress, hydrogen peroxide and other free radical species that harm cellular lipids, proteins, and DNA, hence causing cancer (DesMarias and Costa, 2019).

Several sensors have been employed to monitor Cr levels in the last few years to mitigate its adverse effects. It includes modifying electrode surfaces using various nanomaterials and different biorecognition elements.

Electrochemical biosensors have a wide array of applications for the detection of heavy metals, as already discussed above. Similarly, numerous electrochemical biosensors have also been developed to detect chromium. For instance, natural melanin nanoparticles (MNP) were used to create a biosensor that was embellished with an SPCE (Kaleli-Can et al., 2020). Cr^{6+} was selected as a heavy metal ion to be detected to assess the novel biosensor's performance. The ink of the cuttlefish (*Sepia officinalis*) was used to extract natural MNP. SPCEs were decorated with MNP using two different techniques. The first was layer-by-layer assembly (LBLA) for 'n' no. of varied cycle times. In the second, SPCE was treated with plasma using evaporation-induced self-assembly (EISA) techniques and incubated for a time range in an MNP solution. After evaluating the efficiency of both of the modified SPCEs for amperometric detection of Cr^{6+} in various water samples, the reduction peak of Cr^{6+} was found to occur at 0.33 V. Amperometric measurements of Cr^{6+} for SPCEs modified with 12h-EI-SA and 14n-LBL-A depicted wide linearity in the range of 0.1-5 μM and 0.1-2 μM, respectively. Both modified SPCEs also detected Cr^{6+} in samples of tap and lake water, as well as in a simulated aqueous system constituting different additional heavy metals and minerals. For 12h-EI-SA, the LOD and LOQ values were found to be 0.03 μM and 0.1 μM, respectively. This demonstrated the possibility of MNP-modified SPCEs using EISA techniques to replace conventional detection methods like ICP-MS. Similar to this, a GCE modified with Nafion (g-C_3N_4 /AgM/Nf/GCE) (Karthika et al., 2020) was used to immobilize graphene carbon nitride in another electrochemical sensor for Cr^{6+} detection by Karthika A et al. The schematic has been illustrated in **Figure 4A**. A number of analytical and spectroscopic techniques were used to analyze the nanocomposite after it was generated using a sonochemical procedure. The g-C_3N_4/AgM/Nf/GCE was analyzed using the amperometric method, showing superior electrocatalytic activity with a LOD value as low as 0.0016 μM, the sensitivity of 65.8 μA μM^{-1} cm^{-2}, and LDR between 0.1 and 0.7 μM. The biosensor demonstrated good sensitivity, stability, reproducibility, and selectivity. This electrochemical sensing technique was also used to detect Cr^{6+} in water samples, and it demonstrated excellent viability and recovery. Another series of experiments by Xu Y et al. for developing an electrochemical sensor involved the voltammetric examination of Cr^{6+} using an electrode modified with pyridine-functionalized AuNPs and synthesizing 3-dimensional graphene (Xu et al., 2019). Graphene oxide (GO) was electrochemically reduced on a carbon electrode with a glassy surface, as shown in **Figure 4B**. AuNPs were electrodeposited onto the surface of graphene at a constant voltage, and the self-assembling pyridine group joined with AuNP. The created materials were examined using scanning electron microscopy (SEM), Raman spectroscopy, and electrochemical methods. Each modification stage was examined using CV and electrochemical impedance spectroscopy (EIS). The created electrode showed a significant current response to Cr^{6+} utilizing differential pulse adsorptive stripping voltammetry (DPASV). With a LOD value of 1.16 μg/L, its linear response was achieved under ideal conditions in the concentration ranging from 25 to 300 μg/L. The fabricated electrode also showed excellent repeatability, stability, and selectivity and was used to find Cr^{6+} in real samples.

Along with electrochemical techniques, optical techniques for the detection of Cr were also explored. Porous silicon structures were used as the enzyme immobilization substrate for the efficient detection of Cr in aqueous samples because of their specific optical properties (Biswas et al., 2017). An optical biosensor, through naked-eye visualization of the enzymatic activity of β-galactosidase (β-GAL), was developed by Hossain and Brennan JD. It utilized chlorophenol red β-galactopyranoside, which upon hydrolyzation by β-GAL, formed a red magenta-coloured product as illustrated in **Figure**

Preprints (www.preprints.org) | NOT PEER-REVIEWED | Posted: 15 January 2024 doi:10.20944/preprints202401.1006.v1

4C. Upon subsequent addition of the metal ions to the bioactive paper, a loss in color was observed in a concentration-dependent manner. The LOD value was found to be 0.150 ppm (Hossain and Brennan, 2011). In another study by Duffy G et al., a colorimetric lab-on-a-disc sensor was developed named 'ChromiSense'. This device can be used to detect both, Cr^{3+} and Cr^{6+}. It utilized 2,6-pyridine dicarboxylic acid (for Cr^{3+} detection) and 1,5-diphenyl carbazide (for Cr^{6+} detection) as ligands, respectively (Duffy et al., 2018). The sample (to be tested) and reagents were placed into a reservoir on the disposable microfluidic disc before analysis. The disc was rotated to force liquids through microchannels with centrifugal force, mixing and reacting to produce a colourful product. The coloured product was then studied under an inexpensive optical detection setup where absorbance readings could be tracked continuously. A photodiode (PD) and light emitting diode (LED) couple comprised the optical detection system. The LDR and LOD for Cr^{3+} using this device were reported to be 69-1000 mg L^{-1} and 21 mg L^{-1}, respectively, whereas those for Cr^{6+} were 14-1000 µg L^{-1} and 4 µg L^{-1}, respectively.

Some other biosensors have also been reported over time and are enlisted in **Table 4.** The sensing molecule, fabrication strategy, detection method, LDR, LOD, and real sample data have been mentioned precisely.

Preprints (www.preprints.org) | NOT PEER-REVIEWED | Posted: 15 January 2024 doi:10.20944/preprints202401.1006.v1

Table 4. List of biosensors for detection of Chromium (NR-Not reported).

S.No.	Sensing molecule	Method of detection	Fabrication Strategy	LDR	LOD	Real Sample	Reference
1	Chromium	DPV, EIS	AgNPs-BP-BPQ NRs prepared and used as a modifier for the preparation of modified graphite paste electrodes	Tap water, river water, waste water	8×10^{-11} M-1×10^{-8} M (tap water) 10^{-8} M-10^{-6} M (river water) 10^{-6}M-10^{-4}M (waste water)	2×10^{-12} M	(Shahbakhsh and Noroozifar, 2019)
2	Chromium	CV	Nickel oxide nanoparticles coated on a fluorine-doped tin oxide plate for Cr detection.	NR	NR	5 ppM-50 ppM	(Kowsalya et al., 2019)
3	Chromium	DPASV	Ag-plated GCE was used for the detection	Tap water	0.35 µM-40 µM	0.10 µM	(Stojanović et al., 2018)
4	Chromium	DPCASV	Bismuth film electrode prepared with a reversibly deposited mediator (Zn)	Sea water, estuarine water, rain water, river water	0.0002 nmol/L-0.00125 nmol/L	0.000058 nmol/L	(Tyszczuk-Rotko et al., 2018)
5	Chromium	CV, Chronoamperometry	Glucose oxidase (GO_x) immobilized paper implanted screen	NR	0.05 ppM-1 ppM	0.05 ppM	(Dabhade et al., 2021)

Preprints (www.preprints.org) | NOT PEER-REVIEWED | Posted: 15 January 2024 doi:10.20944/preprints202401.1006.v1

			printed carbon electrode' (SPCE)				
6	Chromium	LSV	Gold nanostars (AuNSs) modified carbon paste screen printed electrodes (CPSPE) were used	Well water	10 ppb-75000 ppb	3.5 ppb	(Dutta et al., 2019)
7	Chromium	DPV	Unmodified carbon paste electrode used in an acidic medium containing DPC.	Tap water	50 µg/L-260 µg/L	19 µg/L	(Hilali et al., 2018)
8	Chromium	LSV	Screen printed electrode modified with gold nanoparticles (AuNPs-SPCE) to form a miniaturized portable electrochemical system	River water	20 µg/L-200 µg/L	5.4 µg/L	(Tu et al., 2018)
9	Chromium	EIS, SWV	Immobilization of β-GAL on electrochemical transducer by crosslinking with glutaraldehyde and	River water	2.94×10^{-2} µg/L – 2.94×10^{4} µg/L by both EIS, SWV	91.7ng/L by both EIS, SWV	(Fourou et al., 2016)

Preprints (www.preprints.org) | NOT PEER-REVIEWED | Posted: 15 January 2024 doi:10.20944/preprints202401.1006.v1

			detection is based on inhibition of β-GAL by Cr				
10	Chromium	Linear Sweep Anodic stripping voltammetry (LSASV)	Fabrication of Gold Nanoparticles on screen-printed electrodes to detect Cr	Tap and sea water	0.7 µg/L- 35 µg/L	1.6 pg/mL	(Tukur et al., 2015)
11	Chromium (III) and (VI)	DPCSV, CV	Carbon paste electrode modified with Citrobacter freundii (Cf-CPE) to detect Cr^{3+} and Cr^{6+}	Chromite mine water	NR	Cr (VI) DPCSV-1×10^{-9} M Cr (III) DPCSV-1×10^{-7} M Cr (VI) CV-1×10^{-4} M Cr (III) CV- 5×10^{-4} M	(Prabhakaran et al., 2017)
12	Chromium	CV	NR	Water	25 µM to 1 mM	LOD	(Stern et al., 2020)
13	Chromium	Luminescence detection	Luminescent carbon dots (CDs) from indigenous potato sources	Water	0.5 µM–100 µM	0.012 µM	(Sinha et al., 2020)

List of abbreviations: DPV- Differential Pulse Voltammetry, DPASV – Differential Pulse Anodic Stripping Voltammetry, DPCSV – Differential Pulse Cathodic Stripping Voltammetry, CV- Cyclic Voltammetry, LSV – Linear Sweep Voltammetry, EIS – Electrochemical Impedance Spectroscopy, SWV- Square Wave Voltammetry, DPI- Dual Polarization Interferometry, GCE – Glassy Carbon Electrode, MWCNT- Multi-Walled Carbon Nanotubes, DMOAP -N, N-dimethyl-N-octadecyl-3-aminopropyltrimethoxysilyl chloride, APTES- (3-aminopropyl) triethoxysilane (3-APTES), GA-Glutaraldehyde, DPC- 1,5-Diphenylcarbazide.

Preprints (www.preprints.org) | NOT PEER-REVIEWED | Posted: 15 January 2024 doi:10.20944/preprints202401.1006.v1

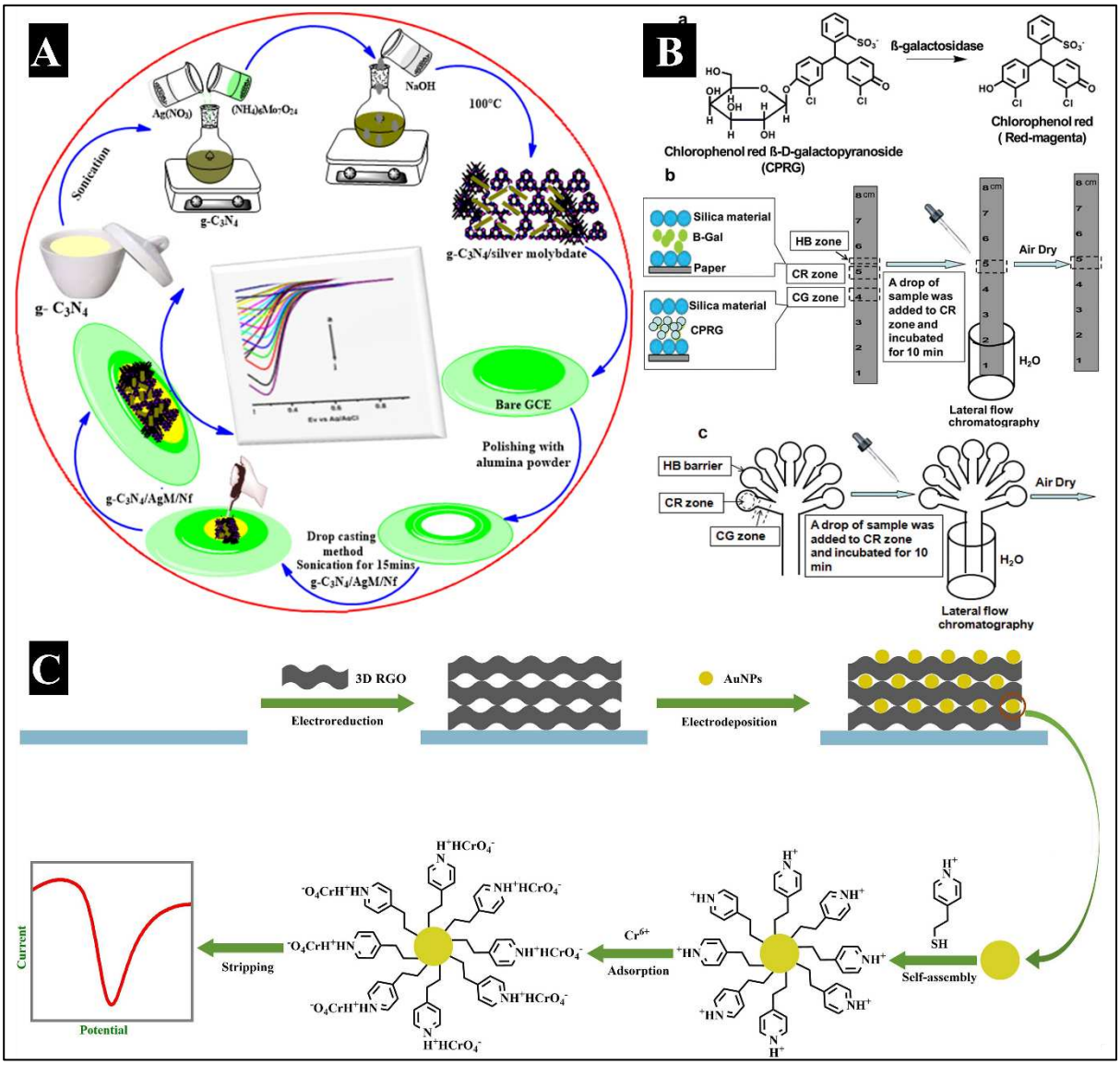

Figure 4. A) Step-by-step fabrication of GCE with g-C3N4/AgM/Nf modification for Cr^{6+} detection (adapted with permission from (Karthika et al., 2020); B) Schematic showing the process for creating pyridine-functionalized AuNPs in 3D RGO/GCE for analysing Cr^{6+} (adapted with permission from (Hossain and Brennan, 2011); C) Diagram illustrating the two sensor designs and the detection mechanism for detecting heavy metal ions (adapted with permission from (Xu et al., 2019).

Biosensors for the detection of nickel

Ni represents the second most abundant element within the earth and one of the common elements (24th in order) present in the earth's crust. Although it exists in a number of oxidation states from -1 to +4, the +2-oxidation state is the most prevalent in the biosphere. It is distributed in the environment due to volcanic eruptions, erosions, and meteorites. Aqueous Ni comes from biological processes and the solubilization of Ni compounds in soils. According to the WHO and the EPA, the maximum concentration of Ni in environmental waters should not exceed 0.07 and 0.04 ppm, respectively (Aragay et al., 2011). Apart from the natural occurrence, anthropogenic activities like emissions from fossil fuel consumption, Ni refining, electroplating, welding, alloy production, and several metallurgical activities also lead to its accumulation in the environment. As a result, it is present naturally in food and water. As it promotes hormonal activity and is involved in lipid metabolism, Ni is also classified as a micronutrient, crucial for the human body to function properly. It can be ingested, inhaled, or absorbed via the skin. A number of chronic health effects, such as

 doi:10.20944/preprints202401.1006.v1

allergies, lung fibrosis, contact dermatitis, cardiovascular diseases, and renal diseases, are triggered by prolonged contact with nickel, even at relatively low concentrations (Antico and Soana, 2015; Denkhaus and Salnikow, 2002; Genchi et al., 2020). Additionally, several Ni compounds (such as Ni sulphides and Ni oxides) have also been reported to be carcinogenic and found to be associated with respiratory tract cancers (Goodman et al., 2009; States, 2017). This is attributed to the fact that prolonged Ni exposure is the most frequent and common reason for cancer.

The molecular mechanism of Ni and Ni compound-induced DNA damage associated with carcinogenesis has been extensively studied. The precise processes by which Ni and Ni compounds harm DNA remain unknown. Previous research has shown that Ni can cause DNA damage and that this damage is mostly caused by the formation of reactive oxygen species (ROS). Ni can also attach to DNA directly and cause DNA damage. The accumulation of damaged DNA bases is accelerated by Ni's ability to suppress DNA damage repair mechanisms, including DNA direct-reversal, nucleotide repair (NER), base excision repair (BER), mismatch repair (MMR), and non-homologous end joining (NHEJ) repair pathways. The reduction of direct enzyme activity as well as the manipulation of DNA repair molecule expression is two methods by which cellular DNA repair is suppressed. As a result, exposure to nickel can cause cancer directly by damaging DNA and impairing DNA repair. On the other side, Ni can indirectly increase the risk of cancer when combined with other cancer-causing agents (such as ionizing radiation, chemicals, and UV light). Damaged DNA accumulates in the cells as a result of Ni-induced DNA repair pathway inhibition. If the DNA-damaged cell survives, the damaged DNA is passed on to daughter cells through the damage site, which may lead to the development of cancer. Workers who work with nickel suffer very substantial DNA damage. Numerous human cell systems, including human hepatocellular carcinoma (HepG2), human TK6, Chinese hamster lung fibroblast A375 and HCT-116 cells, were also reported to be susceptible to DNA damage caused by Ni^{2+} in earlier investigations (Guo et al., 2019).

Therefore, measuring nickel intake is crucial due to its negative consequences on human health. This is a public health issue that needs to be quickly and effectively monitored by testing. Health concerns due to such trace elements have thus sparked growing attention towards the advancement and deployment of biosensors for food analysis applications (Mishra et al., 2018; Neethirajan et al., 2018; Taher et al., 2014).

Electrochemical biosensors offer a wide range of benefits due to their ability to recognize certain targets with great selectivity and affinity. The common synthetic ligand used for most nickel biosensors is dimethylglyoxime (DMG). It has been used as a Ni^{2+} ion chelator for selective chemical detection using techniques such as adsorptive cathodic square-wave stripping voltammetry and cathodic stripping voltammetry (González et al., 2002; Mettakoonpitak et al., 2017). Interfering ions often have a limited impact because of the unique reaction between Ni^{2+} ions and DMG. A simple electrochemical approach involving DMG was crafted for rapid, real-time detection of Ni^{2+} ions in discharged water from mines (Ferancová et al., 2016). The carbon paste electrode (CPE) was modified using DMF, and DMG/CPE porous structure was obtained. It was optimized using the DPV procedure and has a LOD value of 0.027 mg L^{-1} and a linear range of 0.08 to 0.6 mg L^{-1}. Similarly, Ni in fuel ethanol was measured using a mercury-free electrode that had been chemically treated using carbon paste containing DMG (Tartarotti et al., 2006). An electrochemical biosensor was developed by Yang et al. for the detection of Ni^{2+} ions using DNAzyme-CdSe nanocomposite as the bioreceptor (Yang et al., 2016). It was obtained by hybridizing the thiol-containing enzyme strand (DNA1) with its substrate DNA strand having an amino group (DNA2) on the gold electrode and subsequent incorporation of CdSe quantum dots (QD's) by covalent assembling, as shown in **Figure 5A**. In the Ni^{2+} ions' presence, the substrate strand of the enzyme, DNAzyme, gets catalytically cleaved, thus forming smaller DNA fragments containing CdSe QDs. DPASV was then used for the detection of remaining QDs on the electrode surface. Thus, high sensitivity and selectivity were obtained for the detection of Ni^{2+} ions with linearity from 20 nM to 0.2 mM and a low LOD of 6.67 nM. Recently, a miniaturized and flexible sensor for the sensitive, accurate, and rapid detection of Ni^{2+} ions was developed by Elashery et al. using a potentiometric technique (Elashery et al., 2022). The sensor was designed using highly porous and flexible activated carbon cloth (AFCC), doped with polypyrrole

 doi:10.20944/preprints202401.1006.v1

nanoparticles (PNP), collectively referred to as AFCC-PNP. The fabrication is shown in **Figure 5B**. It acted as the wearable substance, with 2D Ni-MOF nanosheets as the electroactive material. This sensor detected Ni^{2+} ions without any preconditioning within biological fluids such as saliva and sweat as well as environmental samples with a LOD of 2.7×10^{-6} mol L^{-1}. Furthermore, the sensor showed remarkable antibacterial properties against the growth of both gram-positive and gram-negative bacteria, making it suitable for use as a wearable sensor.

Apart from electrochemical sensors, optical detection techniques for Ni^{2+} ions were also explored. Alizadeh et al. reported the use of an ionophore having O and N as atom donors for the development of an optical sensor, which was highly selective for targeting Ni^{2+} (Alizadeh et al., 2014). It was achieved by covalently immobilizing 1-p-tolyl-3-(3-(trifluoromethyl) phenyl) triaz-1-ene1-oxide upon a transparent triacetyl cellulose membrane. Studies revealed a significantly higher stability constant for the Ni ion-triazene-1-oxide complex in acetonitrile solution when compared with other metal ions. The membrane sensor, thus produced, exhibited a linearity between 1.18×10^{-9} – 7.34×10^{-5} M for Ni^{2+} ion concentration at pH 5.7. The LOD for this method of Ni^{2+} ion detection was found to be 1.0×10^{-9} M. Another example of colorimetric sensor for Ni detection was presented by Kang et al. The sensor molecule was synthesized by combining 5(4)-amino-4(5)-(aminocarbonyl)-imidazolehydrochloride with 2-pyridine-carboxaldehyde (Kang et al., 2017). Upon Ni^{2+} presence in an aqueous solution, a distinctive color change occurred from colorless to yellow, thus making naked-eye detection possible. The LOD was 57 nM, much below the EPA guidelines for Ni^{2+} ions.

Different nanomaterials have also been utilized for colorimetric detection of Ni. For example, citrate-stabilized silver nanoparticles (AgNPs), glutathione and cysteine-modified silver nanoplates (AgNPls) and N-cholyl-L-valine (NaValC)-capped AuNPs (as shown in **Figure 5C**) have been shown to exhibit extremely high selectivity towards Ni^{2+} over others under specific conditions (Annadhasan et al., 2015; He et al., 2021; Kiatkumjorn et al., 2014). The mechanism behind the detection ability of these nanomaterials was that under optimum conditions, Ni^{2+} ions induced aggregation of the nanoparticles through the metal-ligand interaction arising between the capping ligands and Ni^{2+}, resulting in a distinctive observable color change. This was confirmed by transmission electron microscopy (TEM) images showing the increase in the hydrodynamic radius along with a significant change from negative to positive values as indicated by zeta potential analysis.

Many of the other reported biosensors have also been enlisted in **Table 5,** where the sensing molecule, fabrication strategy, detection method, LDR, LOD, and real sample data have been mentioned precisely.

Preprints (www.preprints.org) | NOT PEER-REVIEWED | Posted: 15 January 2024 doi:10.20944/preprints202401.1006.v1

Table 5. List of biosensors for detection of Nickel (NR-Not reported).

S.No.	Sensing molecule	Method of detection	Fabrication Strategy	Real sample	LDR	LOD	Reference
1	Nickel	DPASV	Biosensor based on CdSe QDs, enzyme strand (DNA 1) and substrate strand (DNA 2). The substrate strand would be cleaved in the presence of Ni^{2+}	NR	20 nM-0.2 mM	6.67 nM	(Yang et al., 2016)
2	Nickel	DPV	DMG-modified CPE developed to detect Ni (II)	Mine water	0.08-0.6 mg/L	0.027 mg/L	(Ferancová et al., 2015)
3	Nickel	CV	Mn_3O_4-Chitosan nanocomposite-modified platinum electrodes developed	The aqueous solution, Tap water, lake water	5- 250 µg/L	0.718 µg/L	(John and Abraham, 2021)
4	Nickel	Optical	Immobilization of triazene-1-oxide derivatives on a triacetylcellulose membrane	Spring water, River water	1.18×10^{-9}-7.34×10^{-5} M	1×10^{-9} M	(Alizadeh et al., 2014)
5	Nickel	Colorimetric	Sunlight-induced green synthesis of AuNPs and used for colorimetric detection	Tap water, Drinking water	5-40 nM	10 nM	(Annadhasan et al., 2015)
6	Nickel	AASV	CPE modified with cation exchanger Dowex	Tap water, Mineral water	NR	0.005 µg/L	(González et al., 2002)
7	Nickel	Colorimetric	Colorimetric chemical sensor synthesized from the combination of 5(4)-amino-4(5)-(aminocarbonyl)-imidazole hydrochloride and 2-pyridine-carboxaldehyde.	Tap water, Drinking water, sewage water	0-10 µM	0.057 µM	(Kang et al., 2017)
8	Nickel	Colorimetric	Glutathione and cysteine-modified nanoplates developed (GSH-Cys-AgNPls),	Waste samples	10-150 ppb	7.02 ppb	(Kiatkumjorn et al., 2014)

			SPR peak was observed in accordance with a change in Ni (II) level				
9	Nickel	Colorimetric	Functionalization of trisodium citrate as a stabilizer to detect nickel on the surface of silver nanoparticles	Tap water	0.7-1.6 mM	0.75 mM	(Almaquer et al., 2019)
11	Nickel	DPV	A carbon paste containing dimethylglyoxime chemically applied upon a Hg-free electrode	Fuel sample	1.1×10^{-8}-6.9×10^{-8} M	2.7×10^{-9} M	(Tartarotti et al., 2006)
12	Nickel	Potentiometric	Flexible activated carbon fabric decorated with nitrogen gas and spherical porous carbon nanoparticles coated with 2D Ni-MOF nanosheets	Saliva, sweat, tap water	1.0×10^{-5} -1.0×10^{-1} mol L^{-1}	2.7×10^{-6} mol L^{-1}	

List of abbreviations: DPASV – Differential Pulse Anodic Stripping Voltammetry, DPV- Differential Pulse Voltammetry, CV- Cyclic Voltammetry, AASV- Adsorptive Anodic Stripping Voltammetry, DPCSV – Differential Pulse Cathodic Stripping Voltammetry, QDs- Quantum Dots, CPE- Carbon Paste Electrode, DMG- Dimethylglycine.

Preprints (www.preprints.org) | NOT PEER-REVIEWED | Posted: 15 January 2024 doi:10.20944/preprints202401.1006.v1

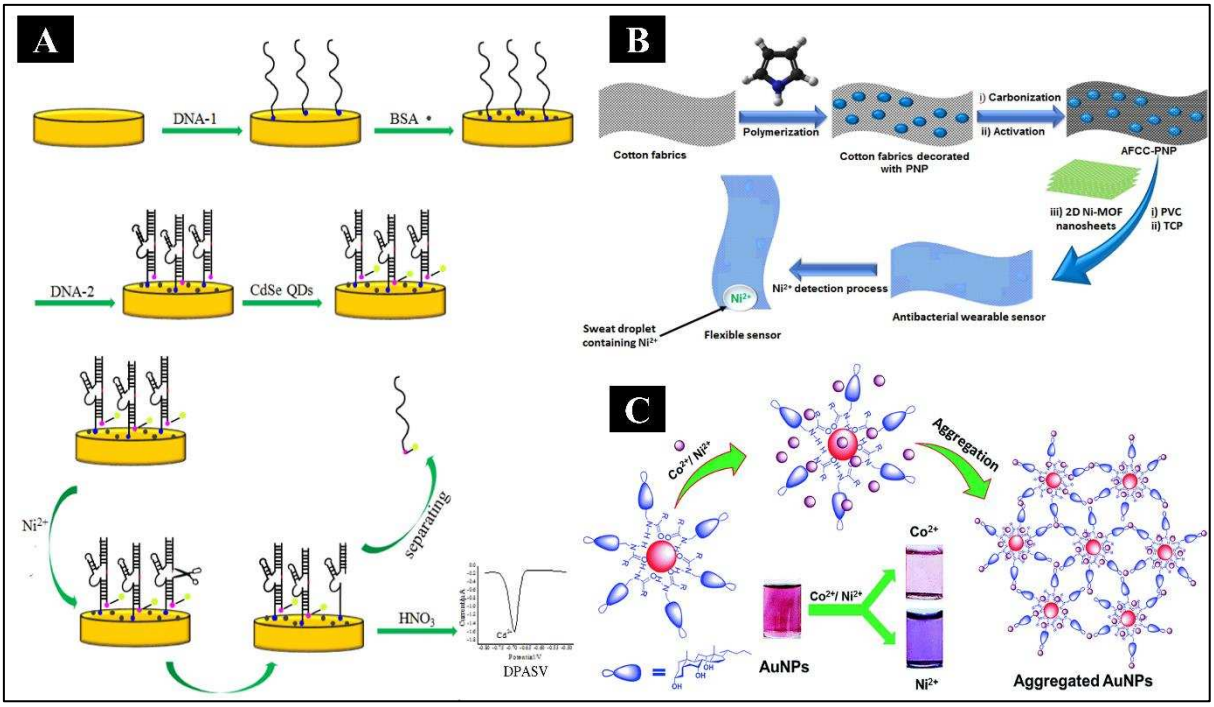

Figure 5. A) Electrochemical biosensor preparation process and a step-by-step experimentation approach (adapted with permission from (Yang et al., 2016); B) A schematic showing the creation of the AFCC-PNP and its 2D Ni-MOF nanosheet-based flexible antibacterial sensor (adapted with permission from (Elashery et al., 2022); C) Gold nanoparticles (green synthesis) fabrication and their utilization in colorimetric detection of ions like Ni^{2+} and Co^{2+} (adapted with permission from (Annadhasan et al., 2015).

Conclusion

Carcinogenic metals are widely distributed in the environment due to emissions from numerous domestic, medical, industrial, agricultural, and technical setups. Its possible environmental and human health consequences could be catastrophic in the long run. As, Be, Cd, Cr, and Ni are the five frontrunner metals raising serious public health concerns due to their high degree of toxicity. Even at low concentrations, these metallic elements are known to cause damage to various organs and are regarded as carcinogens. Their detection has been a major area of research for a long time. Several methods have been developed over time, evolving day by day. This paper has explicitly tried to cover all the biosensors which have been developed so far for the detection of these carcinogens. These include electrochemical biosensors with different electrode modifications, optical or colorimetric biosensors, paper-based biosensors, carbon nanotube-based biosensors, whole cell biosensors, bacterial biosensors, microcantilever biosensors, and hydrogel biosensors. All these devices have tried to keep their LOD values as low as possible and are competing in selectivity, sensitivity, stability, and durability. Most have been run over real contaminated water samples from different sources to detect the carcinogen quantity.

Despite all the advancements and low LOD values, these biosensors need to be commercialized at the industrial level, combining good features of all. But limited information is there on the detection time of these reported biosensors, which needs to be revealed for public information and utilization. Also, the fabrication steps of these biosensors can be simplified, making them more cost-effective. This review paper has comprehensively tried to cover the mechanisms of metal carcinogenicity and types of biosensors developed throughout the world for carcinogenic metal detection, with thorough information on their fabrication and analytical values. There is no such literature reported anywhere throughout to do so, to the best of our knowledge. This can be a boon for commercializing biosensors to detect carcinogenic metals.

Authors Contribution: Akanksha Singh: Conceptualization, Analysis, Visualization, Investigation, Writing-original draft, Writing review and editing; Writing review and editing.

Funding: Not applicable.

Acknowledgements: Akanksha Singh is thankful to the Ministry of Human Resource and Development (MHRD), India, for financial aid in the form of fellowship. A sincere thanks to Indrajeet Yadav, School of Biochemical Engineering, Indian Institute of Technology (BHU) Varanasi, for his valuable suggestions.

Competing Interests: The authors hereby declare that they have no known competing financial interest or personal relationships that could have influenced the reported study in this paper.

References

1. Alhadrami, H.A., 2018. Biosensors: Classifications, medical applications, and future prospective. Biotechnol. Appl. Biochem. 65, 497–508. https://doi.org/10.1002/bab.1621
2. Alizadeh, K., Rezaei, B., Khazaeli, E., 2014. A new triazene-1-oxide derivative, immobilized on the triacetyl cellulose membrane as an optical Ni2+ sensor. Sensors Actuators, B Chem. 193, 267–272. https://doi.org/10.1016/j.snb.2013.11.061
3. Almaquer, F.E.P., Ricacho, J.S.Y., Ronquillo, R.L.G., 2019. Simple and rapid colorimetric sensing of Ni(II) ions in tap water based on aggregation of citrate-stabilized silver nanoparticles. Sustain. Environ. Res. 1. https://doi.org/10.1186/s42834-019-0026-3
4. Annadhasan, M., Kasthuri, J., Rajendiran, N., 2015. Green synthesis of gold nanoparticles under sunlight irradiation and their colorimetric detection of Ni2+ and Co2+ ions. RSC Adv. 5, 11458–11468. https://doi.org/10.1039/c4ra14034f
5. Antico, A., Soana, R., 2015. Nickel Sensitization and Dietary Nickel are a Substantial Cause of Symptoms Provocation in Patients with Chronic Allergic-Like Dermatitis Syndromes. Allergy Rhinol. 6, ar.2015.6.0109. https://doi.org/10.2500/ar.2015.6.0109
6. Aoshima, K., 2016. Itai-itai disease: Renal tubular osteomalacia induced by environmental exposure to cadmium—historical review and perspectives. Soil Sci. Plant Nutr. 62, 319–326. https://doi.org/10.1080/00380768.2016.1159116
7. Aragay, G., Pons, J., Merkoçi, A., 2011. Recent trends in macro-, micro-, and nanomaterial-based tools and strategies for heavy-metal detection. Chem. Rev. 111, 3433–3458. https://doi.org/10.1021/cr100383r
8. Azad, U.P., Mahapatra, S., Divya, Chandra, P., Srivastava, A., Shetti, N.P., 2022. Electrochemical biosensors for monitoring of bioorganic and inorganic chemical pollutants in biological and environmental matrices. Microb. Biodegrad. Bioremediation Tech. Case Stud. Environ. Pollut. 509–531. https://doi.org/10.1016/B978-0-323-85455-9.00001-1
9. Beiraghi, A., Babaee, S., Roshdi, M., 2011. A selective optical sensor for beryllium determination based on incorporating of 1,8-dihydroxyanthrone in a poly (vinyl chloride) membrane. J. Hazard. Mater. 190, 962–968. https://doi.org/10.1016/j.jhazmat.2011.04.033
10. Beyersmann, D., Hartwig, A., 2008. Carcinogenic metal compounds: Recent insight into molecular and cellular mechanisms. Arch. Toxicol. 82, 493–512. https://doi.org/10.1007/s00204-008-0313-y
11. Biswas, P., Karn, A.K., Balasubramanian, P., Kale, P.G., 2017. Biosensor for detection of dissolved chromium in potable water: A review. Biosens. Bioelectron. 94, 589–604. https://doi.org/10.1016/j.bios.2017.03.043
12. Bustaffa, E., Stoccoro, A., Bianchi, F., Migliore, L., 2014. Genotoxic and epigenetic mechanisms in arsenic carcinogenicity. Arch. Toxicol. 88, 1043–1067. https://doi.org/10.1007/s00204-014-1233-7
13. Cai, Y., Zhu, K., Shen, L., Ma, J., Bao, L., Chen, D., Wei, L., Wei, N., Liu, B., Wu, Y., Chen, S., 2022. Evolved Biosensor with High Sensitivity and Specificity for Measuring Cadmium in Actual Environmental Samples. Environ. Sci. Technol. 56, 10062–10071. https://doi.org/10.1021/acs.est.2c00627
14. Chakraborty, S., Dutta, A.R., Sural, S., Gupta, D., Sen, S., 2013. Ailing bones and failing kidneys: A case of chronic cadmium toxicity. Ann. Clin. Biochem. 50, 492–495. https://doi.org/10.1177/0004563213481207
15. Chandra, P., Noh, H.B., Pallela, R., Shim, Y.B., 2015. Ultrasensitive detection of drug resistant cancer cells in biological matrixes using an amperometric nanobiosensor. Biosens. Bioelectron. 70, 418–425. https://doi.org/10.1016/j.bios.2015.03.069
16. Chandra, P., Noh, H.B., Shim, Y.B., 2013. Cancer cell detection based on the interaction between an anticancer drug and cell membrane components. Chem. Commun. 49, 1900–1902. https://doi.org/10.1039/c2cc38235k
17. Chandra, P., Suman, P., 2021. Immunodiagnostic Technologies from Laboratory to Point-Of-Care Testing, Springer, Singapore. Springer, Singapore. https://doi.org/10.1007/978-981-15-5823-8

18. Chen, D., Yang, M., Zheng, N., Xie, N., Liu, D., Xie, C., Yao, D., 2016. A novel aptasensor for electrochemical detection of ractopamine, clenbuterol, salbutamol, phenylethanolamine and procaterol. Biosens. Bioelectron. 80, 525–531. https://doi.org/10.1016/j.bios.2016.01.025
19. Chen, Q.Y., DesMarais, T., Costa, M., 2019. Metals and mechanisms of carcinogenesis. Annu. Rev. Pharmacol. Toxicol. https://doi.org/10.1146/annurev-pharmtox-010818-021031
20. Dabhade, A., Jayaraman, S., Paramasivan, B., 2021. Development of glucose oxidase-chitosan immobilized paper biosensor using screen-printed electrode for amperometric detection of Cr(VI) in water. 3 Biotech 11. https://doi.org/10.1007/s13205-021-02736-5
21. Deng, S., Jiang, Q., Zhang, T., Xiong, X., Chen, P., 2015. Liquid Crystal Biosensor Based on Cd²⁺ Inducing the Bending of PS-Oligo for the Detection of Cadmium. Health (Irvine. Calif). 07, 986–993. https://doi.org/10.4236/health.2015.78116
22. Denkhaus, E., Salnikow, K., 2002. Nickel essentiality, toxicity, and carcinogenicity. Crit. Rev. Oncol. Hematol. 42, 35–56. https://doi.org/10.1016/S1040-8428(01)00214-1
23. DesMarias, T.L., Costa, M., 2019. Mechanisms of chromium-induced toxicity. Curr. Opin. Toxicol. 14, 1–7. https://doi.org/10.1016/j.cotox.2019.05.003
24. Duffy, G., Maguire, I., Heery, B., Gers, P., Ducrée, J., Regan, F., 2018. ChromiSense: A colourimetric lab-on-a-disc sensor for chromium speciation in water. Talanta 178, 392–399. https://doi.org/10.1016/j.talanta.2017.09.066
25. Dutta, S., Strack, G., Kurup, P., 2019. Gold nanostar-based voltammetric sensor for chromium(VI). Microchim. Acta 186. https://doi.org/10.1007/s00604-019-3847-1
26. Dwivedi, A., Srivastava, M., Upadhyay, R., Srivastava, A., Yadav, R.S., Srivastava, S.K., 2022. A flexible Eu:Y2O3-polyvinyl alcohol photoluminescent film for sensitive and rapid detection of arsenic ions. Microchem. J. 172, 106969. https://doi.org/10.1016/j.microc.2021.106969
27. Ebrahimi, M., Raoof, J.B., Ojani, R., 2018. Design of an electrochemical DNA-based biosensor for selective determination of cadmium ions using a DNA hybridization indicator. Int. J. Biol. Macromol. 108, 1237–1241. https://doi.org/10.1016/j.ijbiomac.2017.11.023
28. Elashery, S.E.A., Attia, N.F., Oh, H., 2022. Design and fabrication of novel flexible sensor based on 2D Ni-MOF nanosheets as a preliminary step toward wearable sensor for onsite Ni (II) ions detection in biological and environmental samples. Anal. Chim. Acta 1197, 339518. https://doi.org/10.1016/j.aca.2022.339518
29. Elcin, E., Öktem, H.A., 2020. Inorganic Cadmium Detection Using a Fluorescent Whole-Cell Bacterial Bioreporter. Anal. Lett. 53, 2715–2733. https://doi.org/10.1080/00032719.2020.1755867
30. Ferancová, A., Hattuniemi, M.K., Sesay, A.M., Räty, J.P., Virtanen, V.T., 2016. Elektrochemisches Monitoring von Nickel (II) in Grubenwasser. Mine Water Environ. 35, 547–552. https://doi.org/10.1007/s10230-015-0357-1
31. Ferancová, A., Hattuniemi, M.K., Sesay, A.M., Räty, J.P., Virtanen, V.T., 2015. Electrochemical Monitoring of Nickel(II) in Mine Water | Elektrochemisches Monitoring von Nickel (II) in Grubenwasser | Monitoreo electroquímico de Ni(II) en agua de mina. Mine Water Environ. https://doi.org/10.1007/s10230-015-0357-1
32. Fourou, H., Zazoua, A., Braiek, M., Jaffrezic-Renault, N., 2016. An enzyme biosensor based on beta-galactosidase inhibition for electrochemical detection of cadmium (II) and chromium (VI). Int. J. Environ. Anal. Chem. 96, 872–885. https://doi.org/10.1080/03067319.2016.1209659
33. Fu, Z., Xi, S., 2020. The effects of heavy metals on human metabolism. Toxicol. Mech. Methods 30, 167–176. https://doi.org/10.1080/15376516.2019.1701594
34. Genchi, G., Carocci, A., Lauria, G., Sinicropi, M.S., 2020. Ijerph-17-00679-V3.Pdf. Int. J. Environ. Res. Public Health 17, 679–700.
35. González, P., Cortínez, V.A., Fontán, C.A., 2002. Determination of nickel by anodic adsorptive stripping voltammetry with a cation exchanger-modified carbon paste electrode. Talanta 58, 679–690. https://doi.org/10.1016/S0039-9140(02)00381-8
36. Goodman, J.E., Prueitt, R.L., Dodge, D.G., Thakali, S., 2009. Carcinogenicity assessment of water-soluble nickel compounds. Crit. Rev. Toxicol. 39, 365–417. https://doi.org/10.1080/10408440902762777
37. Gronow, M., 1984. Biosensors. Trends Biochem. Sci. 9, 336–340. https://doi.org/10.1016/0968-0004(84)90055-0
38. Guo, H., Liu, H., Wu, H., Cui, H., Fang, J., Zuo, Z., Deng, J., Li, Y., Wang, X., Zhao, L., 2019. Nickel Carcinogenesis Mechanism: DNA Damage. Int. J. Mol. Sci. 20, 1–18. https://doi.org/10.3390/ijms20194690
39. He, M.Y., Lin, Y.J., Kao, Y.L., Kuo, P., Grauffel, C., Lim, C., Cheng, Y.S., Chou, H.H.D., 2021. Sensitive and Specific Cadmium Biosensor Developed by Reconfiguring Metal Transport and Leveraging Natural Gene Repositories. ACS Sensors 6, 995–1002. https://doi.org/10.1021/acssensors.0c02204
40. Hilali, N., Ghanam, A., Mohammadi, H., Amine, A., García-Guzmán, J.J., Cubillana-Aguilera, L., Palacios-Santander, J.M., 2018. Comparison between Modified and Unmodified Carbon Paste Electrodes for Hexavalent Chromium Determination. Electroanalysis 30, 2750–2759. https://doi.org/10.1002/elan.201800505

41. Hossain, S.M.Z., Brennan, J.D., 2011. β-Galactosidase-based colorimetric paper sensor for determination of heavy metals. Anal. Chem. 83, 8772–8778. https://doi.org/10.1021/ac202290d
42. Huang, C., Ke, Q., Costa, M., Shi, X., 2004. Molecular mechanisms of arsenic carcinogenesis. Mol. Cell. Biochem. 255, 57–66. https://doi.org/10.1023/B:MCBI.0000007261.04684.78
43. Huang, Y., Wang, L., Wang, W., Li, T., He, Z., Yang, X., 2019. Current status of agricultural soil pollution by heavy metals in China: A meta-analysis. Sci. Total Environ. 651, 3034–3042. https://doi.org/10.1016/j.scitotenv.2018.10.185
44. Hughes, M.F., Beck, B.D., Chen, Y., Lewis, A.S., Thomas, D.J., 2011. Arsenic Exposure and Toxicology : A Historical Perspective 123, 305–332. https://doi.org/10.1093/toxsci/kfr184
45. Hui, C. ye, Guo, Y., Li, H., Gao, C. xian, Yi, J., 2022. Detection of environmental pollutant cadmium in water using a visual bacterial biosensor. Sci. Rep. 12, 1–11. https://doi.org/10.1038/s41598-022-11051-9
46. Iqbal, M., Shah, M.D., Vun-Sang, S., Okazaki, Y., Okada, S., 2021. The therapeutic potential of curcumin in alleviating N-diethylnitrosamine and iron nitrilotriacetate induced renal cell tumours in mice via inhibition of oxidative stress: Implications for cancer chemoprevention. Biomed. Pharmacother. 139. https://doi.org/10.1016/j.biopha.2021.111636
47. Irvine, G.W., Tan, S.N., Stillman, M.J., 2017. A simple metallothionein-based biosensor for enhanced detection of arsenic and mercury. Biosensors 7. https://doi.org/10.3390/bios7010014
48. Ismail, S., Yusof, N.A., Abdullah, J., Abd Rahman, S.F., 2020. Electrochemical detection of arsenite using a silica nanoparticles-modified screen-printed carbon electrode. Materials (Basel). 13. https://doi.org/10.3390/ma13143168
49. Jaishankar, M., Tseten, T., Anbalagan, N., Mathew, B.B., Beeregowda, K.N., 2014. Toxicity, mechanism and health effects of some heavy metals. Interdiscip. Toxicol. 7, 60–72. https://doi.org/10.2478/intox-2014-0009
50. John, N., Abraham, K.E., 2021. Detection of Selenium and Nickel Metal Ion in Water Using Mn3O4-Cn-Modified Electrode. Int. J. Electrochem. 2021, 1–9. https://doi.org/10.1155/2021/6650542
51. Kaleli-Can, G., Ozlu, B., Özgüzar, H.F., Onal-Ulusoy, B., Kabay, G., Eom, T., Shim, B.S., Mutlu, M., 2020. Natural Melanin Nanoparticle-decorated Screen-printed Carbon Electrode: Performance Test for Amperometric Determination of Hexavalent Chromium as Model Trace. Electroanalysis 32, 1696–1706. https://doi.org/10.1002/elan.202000038
52. Kang, J.H., Lee, S.Y., Ahn, H.M., Kim, C., 2017. A novel colorimetric chemosensor for the sequential detection of Ni2+ and CN− in aqueous solution. Sensors Actuators, B Chem. 242, 25–34. https://doi.org/10.1016/j.snb.2016.11.026
53. Karimi, M., Aboufazeli, F., Zhad, H.R.L.Z., Sadeghi, O., Najafi, E., 2014. Cadmium Ions Determination in Sea Food Samples Using Dipyridyl-Functionalized Graphene Nano-sheet. Food Anal. Methods 7, 669–675. https://doi.org/10.1007/s12161-013-9671-z
54. Karthik, V., Karuna, B., Kumar, P.S., Saravanan, A., Hemavathy, R. V., 2022. Development of lab-on-chip biosensor for the detection of toxic heavy metals: A review. Chemosphere 299, 134427. https://doi.org/10.1016/j.chemosphere.2022.134427
55. Karthika, A., Nikhil, S., Suganthi, A., Rajarajan, M., 2020. A facile sonochemical approach based on graphene carbon nitride doped silver molybdate immobilized nafion for selective and sensitive electrochemical detection of chromium (VI) in real sample. Adv. Powder Technol. 31, 1879–1890. https://doi.org/10.1016/j.apt.2020.02.021
56. Kiatkumjorn, T., Rattanarat, P., Siangproh, W., Chailapakul, O., Praphairaksit, N., 2014. Glutathione and l-cysteine modified silver nanoplates-based colorimetric assay for a simple, fast, sensitive and selective determination of nickel. Talanta 128, 215–220. https://doi.org/10.1016/j.talanta.2014.04.085
57. Kowsalya, B., Anusha Thampi, V. V., Sivakumar, V., Subramanian, B., 2019. Electrochemical detection of Chromium(VI) using NiO nanoparticles. J. Mater. Sci. Mater. Electron. 30, 14755–14761. https://doi.org/10.1007/s10854-019-01847-3
58. Kreiss, K., Mroz, M.M., Zhen, B., Wiedemann, H., Barna, B., 1997. Risks of beryllium disease related to work processes at a metal, alloy, and oxide production plant. Occup. Environ. Med. 54, 605–612. https://doi.org/10.1136/oem.54.8.605
59. Kumar, S., Bhanjana, G., Dilbaghi, N., Kumar, R., Umar, A., 2016. Fabrication and characterization of highly sensitive and selective arsenic sensor based on ultra-thin graphene oxide nanosheets. Sensors Actuators, B Chem. 227, 29–34. https://doi.org/10.1016/j.snb.2015.11.101
60. Lay, P.A., Levina, A., 2013. Metal Carcinogens, in: Comprehensive Inorganic Chemistry II (Second Edition): From Elements to Applications. pp. 835–856. https://doi.org/10.1016/B978-0-08-097774-4.00333-8
61. Li, J., Ma, F., Wei, X., Fu, C., Pan, H., 2015a. A highly selective molecularly imprinted electrochemiluminescence sensor for ultra-trace beryllium detection. Anal. Chim. Acta 871, 51–56. https://doi.org/10.1016/j.aca.2015.02.038
62. Li, J., Ma, F., Wei, X., Fu, C., Pan, H., 2015b. A highly selective molecularly imprinted electrochemiluminescence sensor for ultra-trace beryllium detection. Anal. Chim. Acta 871, 51–56. https://doi.org/10.1016/j.aca.2015.02.038

63. Li, Y., Ran, G., Lu, G., Ni, X., Liu, D., Sun, J., Xie, C., Yao, D., Bai, W., 2019. Highly Sensitive Label-Free Electrochemical Aptasensor Based on Screen-Printed Electrode for Detection of Cadmium (II) Ions. J. Electrochem. Soc. 166, B449–B455. https://doi.org/10.1149/2.0991906jes
64. Liu, Y., Lai, Y., Yang, G., Tang, C., Deng, Y., Li, S., Wang, Z., 2017. Cd-aptamer electrochemical biosensor based on AuNPs/CS modified glass carbon electrode. J. Biomed. Nanotechnol. 13, 1253–1259. https://doi.org/10.1166/jbn.2017.2424
65. Liu, Y., Zhang, Dongwei, Ding, J., Hayat, K., Yang, X., Zhan, X., Zhang, Dan, Lu, Y., Zhou, P., 2020. Label-Free and Sensitive Determination of Cadmium Ions Using a Ti-Modified Co3O4-Based Electrochemical Aptasensor. Biosensors 10. https://doi.org/10.3390/bios10120195
66. Lu, H., Wang, P., Tan, R., Yang, X., Shen, Y., 2018. Nanorobotic System for Precise In Situ Three-Dimensional Manufacture of Helical Microstructures. IEEE Robot. Autom. Lett. 3, 2846–2853. https://doi.org/10.1109/LRA.2018.2846051
67. Mahato, K., Kumar, A., Maurya, P.K., Chandra, P., 2018a. Shifting paradigm of cancer diagnoses in clinically relevant samples based on miniaturized electrochemical nanobiosensors and microfluidic devices. Biosens. Bioelectron. 100, 411–428. https://doi.org/10.1016/j.bios.2017.09.003
68. Mahato, K., Maurya, P.K., Chandra, P., 2018b. Fundamentals and commercial aspects of nanobiosensors in point-of-care clinical diagnostics. 3 Biotech. https://doi.org/10.1007/s13205-018-1148-8
69. Mahato, K., Prasad, A., Maurya, P.K., Chandra, P., 2016. Nanobiosensors: Next Generation Point-of-Care Biomedical Devices for Personalized Diagnosis. J. Anal. Bioanal. Tech. https://doi.org/10.4172/2155-9872.1000e125
70. Mandil, R., Prakash, A., Rahal, A., Singh, S.P., Sharma, D., Kumar, R., Garg, S.K., 2020. In vitro and in vivo effects of flubendiamide and copper on cyto-genotoxicity, oxidative stress and spleen histology of rats and its modulation by resveratrol, catechin, curcumin and α-tocopherol. BMC Pharmacol. Toxicol. 21. https://doi.org/10.1186/s40360-020-00405-6
71. Mettakoonpitak, J., Miller-Lionberg, D., Reilly, T., Volckens, J., Henry, C.S., 2017. Low-cost reusable sensor for cobalt and nickel detection in aerosols using adsorptive cathodic square-wave stripping voltammetry. J. Electroanal. Chem. 805, 75–82. https://doi.org/10.1016/j.jelechem.2017.10.026
72. Mishra, G.K., Barfidokht, A., Tehrani, F., Mishra, R.K., 2018. Food safety analysis using electrochemical biosensors. Foods 7. https://doi.org/10.3390/foods7090141
73. Mushiana, T., Mabuba, N., Idris, A.O., Peleyeju, G.M., Orimolade, B.O., Nkosi, D., Ajayi, R.F., Arotiba, O.A., 2019. An aptasensor for arsenic on a carbon-gold bi-nanoparticle platform. Sens. Bio-Sensing Res. 24. https://doi.org/10.1016/j.sbsr.2019.100280
74. Neethirajan, S., Ragavan, V., Weng, X., Chand, R., 2018. Biosensors for sustainable food engineering: Challenges and perspectives. Biosensors 8. https://doi.org/10.3390/bios8010023
75. Nguyen, D.K., Jang, C.H., 2020. Label-free liquid crystal-based detection of As(III) ions using ssDNA as a recognition probe. Microchem. J. 156. https://doi.org/10.1016/j.microc.2020.104834
76. Núñez, C., Triviño, J.J., Arancibia, V., 2021. A electrochemical biosensor for As(III) detection based on the catalytic activity of Alcaligenes faecalis immobilized on a gold nanoparticle–modified screen–printed carbon electrode. Talanta 223. https://doi.org/10.1016/j.talanta.2020.121702
77. O'Sullivan, J.E., Watson, R.J., Butler, E.C.V., 2013. An ICP-MS procedure to determine Cd, Co, Cu, Ni, Pb and Zn in oceanic waters using in-line flow-injection with solid-phase extraction for preconcentration. Talanta 115, 999–1010. https://doi.org/10.1016/j.talanta.2013.06.054
78. Online, V.A., Rahman, M.M., Nagao, Y., Hasnat, M.A., 2018. RSC Advances Electrochemical oxidation of As (III) on Pd immobilized Pt surface : kinetics and sensing 8071–8079. https://doi.org/10.1039/c7ra12576c
79. Pan, J., Li, Q., Zhou, D., Chen, J., 2018. Ultrasensitive aptamer biosensor for arsenic (III) detection based on label-free triple-helix molecular switch and fluorescence sensing platform. Talanta 189, 370–376. https://doi.org/10.1016/j.talanta.2018.07.024
80. Peng, R.P., Xing, L.B., Wang, X.J., Wu, C.J., Chen, B., Ji, H.F., Wu, L.Z., Tung, C.H., 2017. A beryllium-selective microcantilever sensor modified with benzo-9-crown-3 functionalized polymer brushes. Anal. Methods 9, 3356–3360. https://doi.org/10.1039/c7ay00490g
81. Prabhakaran, D.C., Riotte, J., Sivry, Y., Subramanian, S., 2017. Electroanalytical Detection of Cr(VI) and Cr(III) Ions Using a Novel Microbial Sensor. Electroanalysis 29, 1222–1231. https://doi.org/10.1002/elan.201600458
82. Purohit, B., Kumar, A., Mahato, K., Chandra, P., 2020a. Smartphone-assisted personalized diagnostic devices and wearable sensors. Curr. Opin. Biomed. Eng. 13, 42–50. https://doi.org/10.1016/j.cobme.2019.08.015
83. Purohit, B., Vernekar, P.R., Shetti, N.P., Chandra, P., 2020b. Biosensor Nanoengineering: Design, Operation, and Implementation for Biomolecular Analysis. Sensors Int. https://doi.org/https://doi.org/10.1016/j.sintl.2020.100040
84. Qin, J., Dong, B., Cao, L., Wang, W., 2018. Photonic hydrogels for the ultratrace sensing of divalent beryllium in seawater. J. Mater. Chem. C 6, 4234–4242. https://doi.org/10.1039/c8tc00242h

85. Rahman, M.M., Khan, A., Marwani, H.M., Asiri, A.M., 2016. Hydrazine sensor based on silver nanoparticle-decorated polyaniline tungstophosphate nanocomposite for use in environmental remediation 1787–1796. https://doi.org/10.1007/s00604-016-1809-4
86. Ravikumar, A., Panneerselvam, P., Radhakrishnan, K., Christus, A.A.B., Sivanesan, S., 2018. MoS 2 nanosheets as an effective fluorescent quencher for successive detection of arsenic ions in aqueous system. Appl. Surf. Sci. 449, 31–38. https://doi.org/10.1016/j.apsusc.2017.12.098
87. Rousseau, M.-C., Straif, K., Siemiatycki, J., 2005. IARC Carcinogen Update. Environ. Health Perspect. 113. https://doi.org/10.1289/ehp.113-1280416
88. Ruhan, Q., Yinyin, L., Dawei, C., Yushi, G., Zongping, L., Haidong, L., Chengyin, W., 2020. Determination of cadmium ions based on electrochemical DNA biosensors in Rat Tissues. Int. J. Electrochem. Sci. 15, 7347–7358. https://doi.org/10.20964/2020.08.70
89. Saadati, A., Farshchi, F., Hasanzadeh, M., Liu, Y., Seidi, F., 2022. Colorimetric and naked-eye detection of arsenic(iii) using a paper-based colorimetric device decorated with silver nanoparticles. RSC Adv. 12, 21836–21850. https://doi.org/10.1039/d2ra02820d
90. Salimi, A., Mamkhezri, H., Hallaj, R., Soltanian, S., 2008. Electrochemical detection of trace amount of arsenic(III) at glassy carbon electrode modified with cobalt oxide nanoparticles. Sensors Actuators, B Chem. 129, 246–254. https://doi.org/10.1016/j.snb.2007.08.017
91. Sannigrahi, A., Chowdhury, S., Nandi, I., Sanyal, D., Chall, S., Chattopadhyay, K., 2019. Development of a near infrared Au-Ag bimetallic nanocluster for ultrasensitive detection of toxic Pb2+ ions: In vitro and inside cells. Nanoscale Adv. 1, 3660–3669. https://doi.org/10.1039/c9na00459a
92. Sayato, Y., 1989. WHO Guidelines for Drinking-Water Quality. Eisei kagaku 35, 307–312. https://doi.org/10.1248/jhs1956.35.307
93. Shahbakhsh, M., Noroozifar, M., 2019. Ultra-trace determination of hexavalent chromium by novel two dimensional biphenol-biphenoquinone nanoribbons/silver nanoparticles. Sensors Actuators, B Chem. 281, 1023–1033. https://doi.org/10.1016/j.snb.2018.11.060
94. Sharma, P., Bihari, V., Agarwal, S.K., Verma, V., Kesavachandran, C.N., Pangtey, B.S., Mathur, N., Singh, K.P., Srivastava, M., Goel, S.K., 2012. Groundwater Contaminated with Hexavalent Chromium [Cr (VI)]: A Health Survey and Clinical Examination of Community Inhabitants (Kanpur, India). PLoS One 7, 3–9. https://doi.org/10.1371/journal.pone.0047877
95. Sinha, R., Bidkar, A.P., Rajasekhar, R., Ghosh, S.S., Mandal, T.K., 2020. A facile synthesis of nontoxic luminescent carbon dots for detection of chromium and iron in real water sample and bio-imaging. Can. J. Chem. Eng. 98, 194–204. https://doi.org/10.1002/cjce.23630
96. Soleymanpour, A., Rad, N.A., Niknam, K., 2006. New diamino compound as neutral ionophore for highly selective and sensitive PVC membrane electrode for Be2+ ion. Sensors Actuators, B Chem. 114, 740–746. https://doi.org/10.1016/j.snb.2005.06.046
97. Sreekanth, S.P., Alodhayb, A., Assaifan, A.K., Alzahrani, K.E., Muthuramamoorthy, M., Alkhammash, H.I., Pandiaraj, S., Alswieleh, A.M., Van Le, Q., Mangaiyarkarasi, R., Grace, A.N., Raghavan, V., 2021. Multi-walled carbon nanotube-based nanobiosensor for the detection of cadmium in water. Environ. Res. 197, 111148. https://doi.org/10.1016/j.envres.2021.111148
98. States, J.C., 2017. Essential and Non-essential Metals 95–111. https://doi.org/10.1007/978-3-319-55448-8
99. Stern, C.M., Hayes, D.W., Kgoadi, L.O., Elgrishi, N., 2020. Emerging investigator series: Carbon electrodes are effective for the detection and reduction of hexavalent chromium in water. Environ. Sci. Water Res. Technol. 6, 1256–1261. https://doi.org/10.1039/d0ew00146e
100. Stojanović, Z., Koudelkova, Z., Sedlackova, E., Hynek, D., Richtera, L., Adam, V., 2018. Determination of chromium(vi) by anodic stripping voltammetry using a silver-plated glassy carbon electrode. Anal. Methods 10, 2917–2923. https://doi.org/10.1039/c8ay01047a
101. Taghdisi, S.M., Danesh, N.M., Ramezani, M., Sarreshtehdar Emrani, A., Abnous, K., 2018. A simple and rapid fluorescent aptasensor for ultrasensitive detection of arsenic based on target-induced conformational change of complementary strand of aptamer and silica nanoparticles. Sensors Actuators, B Chem. 256, 472–478. https://doi.org/10.1016/j.snb.2017.10.129
102. Taher, M.A., Mazaheri, L., Ashkenani, H., Mohadesi, A., Afzali, D., 2014. Determination of nickel in water, food, and biological samples by electrothermal atomic absorption spectrometry after preconcentration on modified carbon nanotubes. J. AOAC Int. 97, 225–231. https://doi.org/10.5740/jaoacint.12-327
103. Tartarotti, F.O., De Oliveira, M.F., Balbo, V.R., Stradiotto, N.R., 2006. Determination of nickel in fuel ethanol using a carbon paste modified electrode containing dimethylglyoxime. Microchim. Acta 155, 397–401. https://doi.org/10.1007/s00604-006-0638-2
104. Tu, J., Gan, Y., Liang, T., Wan, H., Wang, P., 2018. A miniaturized electrochemical system for high sensitive determination of chromium(VI) by screen-printed carbon electrode with gold nanoparticles modification. Sensors Actuators, B Chem. 272, 582–588. https://doi.org/10.1016/j.snb.2018.06.006

105. Tukur, S.A., Yusof, N.A., Hajian, R., 2015. Linear sweep anodic stripping voltammetry: Determination of Chromium (VI) using synthesized gold nanoparticles modified screen-printed electrode. J. Chem. Sci. 127, 1075–1081. https://doi.org/10.1007/s12039-015-0864-4
106. Tyszczuk-Rotko, K., Madejska, K., Domańska, K., 2018. Ultrasensitive hexavalent chromium determination at bismuth film electrode prepared with mediator. Talanta 182, 62–68. https://doi.org/10.1016/j.talanta.2018.01.053
107. Vega-Figueroa, K., Santillán, J., Ortiz-Gómez, V., Ortiz-Quiles, E.O., Quinones-Colón, B.A., Castilla-Casadiego, D.A., Almodóvar, J., Bayro, M.J., Rodríguez-Martínez, J.A., Nicolau, E., 2018. Aptamer-Based Impedimetric Assay of Arsenite in Water: Interfacial Properties and Performance. ACS Omega 3, 1437–1444. https://doi.org/10.1021/acsomega.7b01710
108. Verma, N., Singh, M., 2005. Biosensors for heavy metals. BioMetals 18, 121–129. https://doi.org/10.1007/s10534-004-5787-3
109. Wang, J., Thongngamdee, S., Lu, D., 2006. Adsorptive stripping voltammetric measurements of trace beryllium at the mercury film electrode. Anal. Chim. Acta 564, 248–252. https://doi.org/10.1016/j.aca.2006.01.100
110. Wang, X., Gao, W., Yan, W., Li, P., Zou, H., Wei, Z., Guan, W., Ma, Y., Wu, S., Yu, Y., Ding, K., 2018. A Novel Aptasensor Based on Graphene/Graphite Carbon Nitride Nanocomposites for Cadmium Detection with High Selectivity and Sensitivity. ACS Appl. Nano Mater. 1, 2341–2346. https://doi.org/10.1021/acsanm.8b00380
111. Wen, S.H., Wang, Y., Yuan, Y.H., Liang, R.P., Qiu, J.D., 2018. Electrochemical sensor for arsenite detection using graphene oxide assisted generation of prussian blue nanoparticles as enhanced signal label. Anal. Chim. Acta 1002, 82–89. https://doi.org/10.1016/j.aca.2017.11.057
112. Xu, Y., Zhang, W., Huang, X., Shi, J., Zou, X., Li, Z., Cui, X., 2019. Adsorptive stripping voltammetry determination of hexavalent chromium by a pyridine functionalized gold nanoparticles/three-dimensional graphene electrode. Microchem. J. 149. https://doi.org/10.1016/j.microc.2019.104022
113. Xue, Y., Wang, Y., Wang, S., Yan, M., Huang, J., Yang, X., 2020. Label-Free and Regenerable Aptasensor for Real-Time Detection of Cadmium(II) by Dual Polarization Interferometry. Anal. Chem. 92, 10007–10015. https://doi.org/10.1021/acs.analchem.0c01710
114. Yadav, R., Kushwah, V., Gaur, M.S., Bhadauria, S., Berlina, A.N., Zherdev, A. V., Dzantiev, B.B., 2020. Electrochemical aptamer biosensor for As3+ based on apta deep trapped Ag-Au alloy nanoparticles-impregnated glassy carbon electrode. Int. J. Environ. Anal. Chem. 100, 623–634. https://doi.org/10.1080/03067319.2019.1638371
115. Yang, L., An, B., Yin, X., Li, F., 2020. ChemComm free electrochemical biosensor for highly sensitive 5311–5314. https://doi.org/10.1039/d0cc01821j
116. Yang, Y., Yuan, Z., Liu, X.P., Liu, Q., Mao, C.J., Niu, H.L., Jin, B.K., Zhang, S.Y., 2016. Electrochemical biosensor for Ni2+ detection based on a DNAzyme-CdSe nanocomposite. Biosens. Bioelectron. 77, 13–18. https://doi.org/10.1016/j.bios.2015.09.014
117. Yavuz, O., Sezen, M., Alcay, Y., Yildirim, M.S., Kaya, K., Ozkilic, Y., Tuzun, N.Ş., Yilmaz, I., 2021. A new perspective on the beryllium sensor platform: Low symmetry phthalocyanine-based molecular design and ultra trace amount Be2+ ion recognition in aqueous media. Sensors Actuators, B Chem. 329, 129002. https://doi.org/10.1016/j.snb.2020.129002
118. Zayed, A.M., Terry, N., 2003. Chromium in the environment: Factors affecting biological remediation. Plant Soil 249, 139–156. https://doi.org/10.1023/A:1022504826342
119. Zeng, L., Gong, J., Rong, P., Liu, C., Chen, J., 2019. A portable and quantitative biosensor for cadmium detection using glucometer as the point-of-use device. Talanta 198, 412–416. https://doi.org/10.1016/j.talanta.2019.02.045
120. Zhang, D., Crini, G., Lichtfouse, E., Rhimi, B., Wang, C., 2020. Removal of Mercury Ions from Aqueous Solutions by Crosslinked Chitosan-based Adsorbents: A Mini Review. Chem. Rec. 20, 1220–1234. https://doi.org/10.1002/tcr.202000073
121. Zhang, J., Fang, J., Duan, X., 2016. Determination of cadmium in water samples by fast pyrolysis-chemical vapor generation atomic fluorescence spectrometry. Spectrochim. Acta - Part B At. Spectrosc. 122, 52–55. https://doi.org/10.1016/j.sab.2016.05.009
122. Zhou, D., Zeng, L., Pan, J., Li, Q., Chen, J., 2020. Autocatalytic DNA circuit for Hg2+ detection with high sensitivity and selectivity based on exonuclease III and G-quadruplex DNAzyme. Talanta 207, 120258. https://doi.org/10.1016/j.talanta.2019.120258
123. Zhou, Y., Tang, L., Zeng, G., Zhang, C., Zhang, Y., Xie, X., 2016. Current progress in biosensors for heavy metal ions based on DNAzymes/DNA molecules functionalized nanostructures: A review. Sensors Actuators, B Chem. 223, 280–294. https://doi.org/10.1016/j.snb.2015.09.090
124. https://www.epa.gov/sdwa/chromium-drinking-water